People's Democratic Republic of Algeria

Ministry of Higher Education and Scientific Research

Mohamed Khider University of Biskra

FACULTY OF EXACT SCIENCES

DEPARTEMENT OF MATHEMATICS

Thesis Submitted in Partial Execution of the Requirements of the Degree of

Master in "**Mathematics**"

Option: Partial Differential Equations and Numerical Analysis

Submitted and Defended By

Sana MADANI

Title :

Biomedical Modeling with Fractional Differential Equations.

Examination Committee Members:

Drs.	Fouzia RADJEH	MKUB	President
Pr.	Tidjani MENACER	MKUB	Supervisor
Drs.	Faiza ZAAMOUNE	MKUB	Examiner

02/06/2025

Dedication

I dedicate the fruits of my humble labor to my dear father, '**chouaib Madani**', who was my first teacher, the first light that illuminated my path, and the lamp that accompanied my steps in the darkness of beginnings. He is the one who planted in my heart the love of knowledge and taught me that success has a path that begins with persistence and that its end is the fruit of tireless effort. You were a constant source of encouragement and prayer for me. I ask God to prolong your life and to make me the delight of your eyes. May you always be a source of pride for me, and may your prayers always be a beacon that never fades.

I express my deep gratitude to my father's wife, or rather the lady who raised me. I thank you for everything you have given me. You are an important part of my life, and your presence has added a lot of beauty and tranquility to our family.

To my brothers **Adam** and **Ahmed**, you were my companions and partners in my academic journey, and I learned a lot from you in all areas of life. Your presence by my side is a great blessing, and I appreciate every moment we spent together in this stage.

To my dear sisters **Souad, Siham, Samah,** and **Amina,** my companions, allies in my journey, and protectors of my dreams, who know my condition and who shared with me the joys of success and the sorrows of challenges. You supported me in moments of weakness and encouraged me in times of achievement, but all my love and gratitude.

To my friends **Hadil, Ghofran, Noura, Nardjess,** and **Maram**, you were my companions in every step and my partners in every challenge and adventure. You shared with me moments of success and failure, and inspired me to persevere and persevere. I dedicate this work to you for your continued presence by my side. I wish you a bright future full of success and achievements.

Acknowledgments

All praise and thanks are due to Allah, who granted me the strength and ability to complete this research work. His guidance has been my support throughout this journey.

I am deeply grateful to my supervisor, Dr. **MENACER Tidjani**, for his continuous support, valuable guidance, and constructive feedback, which were essential in shaping this research.

My sincere thanks go to the examination committee members, Dr. **ZAAMOUNE Faiza** and Dr. **RADJEH Fouzia**, for their time, careful evaluation, and insightful comments.

Special appreciation is extended to Dr. **BERBICHE Mohamed** and Dr. **LAADJAL Baya** for their academic support and significant contributions throughout my studies.

I would also like to thank all my professors who enriched my academic path with their knowledge and guidance.

Finally, I express heartfelt gratitude to my dear colleague **Louamer Hadil** for her constant encouragement, and to everyone who supported me throughout this work.

CONTENTS

LIST OF FIGURES

LIST OF TABLES

NOTATION

- $\mathbb{R}$: set of real numbers.
- $\mathbb{C}$: set of complex numbers.
- $\mathbb{N}$: set of natural numbers.
- I_a^α: Riemann-Liouville fractional Integral.
- D_a^α : Riemann-Liouville fractional derivative.
- ${}_a^C D^\alpha$: Caputo fractional derivative.
- ${}_a^G D^\alpha f(x)$: Grünwald–Letnikov fractional derivative.
- $\Re(\alpha)$: real part of a complex number α.
- $L^1([a,b])$: set of functions that are integrable on the interval $[a,b]$.
- $\Gamma(\cdot)$: Gamma function.
- $\beta(\cdot,\cdot)$: Beta function.
- $E_\alpha(\cdot)$: Mittag-Leffler function.
- $\mathcal{L}\{\cdot\}$: Laplace transform.
- $(f * g)(t)$: Convolution product.
- $\sinh(\cdot), \cosh(\cdot)$: Hyperbolic functions.

INTRODUCTION

Mathematical modeling is an indispensable tool in the modern era, playing a crucial role in understanding and analyzing real-world phenomena across fields such as physics, chemistry, engineering, and biomedical sciences [7] [2]. Despite the common perception that medicine and biology are distant from mathematics, mathematical modeling has provided critical insights into many complex biomedical phenomena, including drug transport within the body, disease spread, and tissue responses to physical stimuli.

Biomedical modeling is a vital branch of mathematical modeling that focuses on developing accurate representations of biological and physiological processes. One of the earliest examples is Daniel Bernoulli's model on smallpox transmission (1760) [2], which was used to evaluate the effectiveness of vaccination and the benefits of immunization, marking an early application of mathematics in medicine.

As knowledge advanced and systems exhibiting nonlinear behaviors and memory-dependent properties emerged, the need for more accurate and flexible mathematical tools became evident [1] [5] [10]. Among the most significant developments in this direction is fractional calculus. This field is a natural extension of classical calculus, offering a more suitable framework to analyze systems with memory effects or cumulative dynamics.

The origin of fractional calculus dates back to the 17^{th} century [14] [8] when Leibniz introduced a notation for the n-th order derivative of a function:

$$\frac{d^n f(x)}{dx^n}$$

In 1695, de L'Hôpital asked the famous question: *"What would the result be if* $n = \frac{1}{2}$*?"* Leibniz replied, *"This is an apparent paradox from which one day useful consequences will be drawn."* This remark is considered the first seed of fractional calculus.

These ideas were further developed beginning in 1730 with Euler, followed by contributions from Lagrange (1772), Fourier, Riemann, Liouville, Grünwald, and others. For a detailed historical progression, To explore the historical evolution of fractional models, refer to [18] [10]

[8].

Leibniz's prediction has been realized in recent decades, as fractional calculus has witnessed significant growth due to its ability to model systems that cannot be accurately represented using classical differential equations, such as anomalous diffusion, viscoelasticity, and pharmacokinetics. Among the pioneers who highlighted biomedical applications of this field is **Bruce J. West**, particularly through his work titled *"Fractional Calculus View of Complexity: Tomorrow's Science"* [19], which presented fractional models that describe biological processes more realistically.

In most subsequent studies, fractional differential equations have shown superior performance compared to classical models in terms of fitting experimental data and predicting the behavior of biomedical systems [4] [11] [16].

This thesis aims to provide a comprehensive overview of modeling biomedical phenomena using fractional differential equations, highlighting the advantages of these models over traditional ones. The work is structured into three main chapters:

- **Chapter 1:** Covers the theoretical foundations of fractional calculus, including key definitions and types of fractional derivatives, and introduces fractional differential equations and solution methods.
- **Chapter 2:** Presents two biomedical models: one describing transdermal drug diffusion using fractional partial differential equations, and another studying predator-prey dynamics in the presence of an infectious disease using fractional ordinary differential equations, along with mathematical analysis and comparison with classical models.
- **Chapter 3:** Focuses on numerical simulations using MATLAB, solving the two models numerically and analyzing results through comparison between fractional and classical models.

Finally, the thesis concludes with a general conclusion that summarizes the main findings and discusses future research directions.

CHAPTER 1

FUNDAMENTALS OF FRACTIONAL CALCULUS

This chapter focuses on the mathematical foundations of fractional calculus, starting with the basic definitions of fractional derivatives and integrals, followed by their properties and key differences from traditional calculus, and concluding with numerical and analytical methods for solving equations involving non-integer order derivatives.

1.1 Fractional Derivatives and Integrals

1.1.1 Riemann-Liouville Fractional Integrals and Fractional Derivatives

1.1.1.1 Riemann-Liouville Fractional Integrals

Let f be a continuous function on the interval [a,b] . An indefinite integral of f is given by the expression:

$$I_a^1 f(x) = \int_a^x f(t)\, dt, \tag{1.1}$$

And for a second indefinite integral, can be expressed as:

$$I_a^2 f(x) = \int_a^x I_a^1 f(s)\, ds = \int_a^x \left(\int_a^s f(t)\, dt \right) ds. \tag{1.2}$$

In general, for any positive integer n, the n-fold integral is defined recursively as:

$$I_a^n f(x) = \underbrace{\int_a^x \int_a^{t_{n-1}} \cdots \int_a^{t_2} \int_a^{t_1}}_{n \text{ times}} f(t_0)\, dt_0\, dt_1 \cdots dt_{n-1}. \tag{1.3}$$

$$I_a^n f(x) = \frac{1}{(n-1)!} \int_a^x (x-s)^{n-1} f(s)\, ds. \tag{1.4}$$

Using the Gamma function, which generalizes factorials to real and complex orders, the fractional integral of order $\alpha \in \mathbb{C}$ with $\Re(\alpha) > 0$ is defined as:

$$I_a^\alpha f(x) = \frac{1}{\Gamma(\alpha)} \int_a^x (x-t)^{\alpha-1} f(t)\, dt, \tag{1.5}$$

.

Definition 1.1.1 *Let $f : [a,b] \to \mathbb{R}$ be a function in $L^1([a,b])$. For any order $\alpha > 0$, the left-sided Riemann–Liouville fractional integral of f is defined by:*

$$I_{a^+}^\alpha f(x) = \frac{1}{\Gamma(\alpha)} \int_a^x (x-t)^{\alpha-1} f(t)\, dt. \tag{1.6}$$

Similarly, the right-sided Riemann–Liouville fractional integral is defined by:

$$I_{b^-}^\alpha f(x) = \frac{1}{\Gamma(\alpha)} \int_x^b (t-x)^{\alpha-1} f(t)\, dt. \tag{1.7}$$

Remark 1.1.1 *In most applications, we use the left-sided Riemann–Liouville fractional integral. However, similar properties hold for the right-sided version as well.*

Property 1.1.1 *Let $f \in L^1([a,b])$, and let $\Re(\alpha) > 0$, $\Re(\beta) > 0$, and $n \in \mathbb{N}$. Then the following properties hold:*

i) $I_{a^+}^\alpha \left(I_{a^+}^\beta f \right)(x) = I_{a^+}^\beta \left(I_{a^+}^\alpha f \right)(x) = I_{a^+}^{\alpha+\beta} f(x)$,

ii) $\lim_{\alpha \to 0^+} I_{a^+}^\alpha f(x) = f(x)$,

iii) $\frac{d}{dx} \left(I_{a^+}^\alpha f \right)(x) = I_{a^+}^{\alpha-1} f(x), \quad$ *for* $\Re(\alpha) > 1$.

For detailed proofs, see [9] and [18].

Example 1.1.1 *We compute the Riemann–Liouville fractional integral of the function $f(x) = x^n$.*

$$I_0^\alpha x^n = \frac{1}{\Gamma(\alpha)} \int_0^x (x-t)^{\alpha-1} t^n\, dt,$$

To evaluate this integral, we apply the change of variables $y = \frac{t}{x}$, under this substitution $dt = x\, dy$, and the limits change from $t = 0$ and $t = x$ to $y = 0$ and $y = 1$, respectively. The *integral becomes:*

$$\begin{aligned}
I_0^\alpha x^n &= \frac{1}{\Gamma(\alpha)} \int_0^x (x-t)^{\alpha-1} t^n \, dt \\
&= \frac{1}{\Gamma(\alpha)} \int_0^1 (x-xy)^{\alpha-1} (xy)^n \cdot x \, dy \\
&= \frac{x^{n+\alpha}}{\Gamma(\alpha)} \int_0^1 (1-y)^{\alpha-1} y^n \, dy \\
&= \frac{x^{n+\alpha}}{\Gamma(\alpha)} B(\alpha, n+1) \\
&= \frac{x^{n+\alpha}}{\Gamma(\alpha)} \cdot \frac{\Gamma(\alpha)\Gamma(n+1)}{\Gamma(\alpha+n+1)} \\
&= \frac{\Gamma(n+1)}{\Gamma(\alpha+n+1)} x^{n+\alpha}.
\end{aligned}$$

1.1.1.2 Riemann–Liouville Fractional Derivatives

Definition 1.1.2 *Let $f \in L^1([a,b])$, and let $n \in \mathbb{N}$ such that $n-1 < \alpha < n$. The left-sided and right-sided Riemann–Liouville fractional derivatives of order α are defined by:*

$$(D_{a^+}^\alpha f)(x) = \frac{d^n}{dx^n} \left(I_{a^+}^{n-\alpha} f \right)(x), \quad \textit{(Left-sided derivative)} \tag{1.8}$$

$$(D_{b^-}^\alpha f)(x) = \left(-\frac{d^n}{dx^n} \right) \left(I_{b^-}^{n-\alpha} f \right)(x). \quad \textit{(Right-sided derivative)} \tag{1.9}$$

Example 1.1.2 *Let $f(x) = x^m$ with $m > -1$, and $g(x) = C$, where C is a constant. For $0 < \alpha < 1$, the Riemann–Liouville fractional derivatives are given by:*

$$(D^\alpha f)(x) = \frac{\Gamma(m+1)}{\Gamma(m-\alpha+1)} x^{m-\alpha},$$

$$(D^\alpha g)(x) = \frac{C}{\Gamma(1-\alpha)} x^{-\alpha}, \qquad (D^{1/2} g)(x) = \frac{C}{\sqrt{\pi x}}.$$

This result shows that the Riemann–Liouville fractional derivative of a constant function is not zero, but rather produces a function that is undefined at $x = 0$.

Property 1.1.2 *Let $f \in L^1([a,b])$, with $\Re(\alpha) > 0$, $\Re(\beta) > 0$, and let $n \in \mathbb{N}$. The following properties of the Riemann–Liouville fractional derivative hold:*

(i) $D_{a^+}^\alpha (I_{a^+}^\alpha f)(x) = f(x)$,

(ii) $D_{a^+}^\beta (I_{a^+}^\alpha f)(x) = I_{a^+}^{\alpha-\beta} f(x)$,

(iii) $D_{a^+}^n (D_{a^+}^\alpha f)(x) = D_{a^+}^{\alpha+n} f(x)$,

(iv) $D_{a^+}^{-\alpha}(D_{a^+}^{\alpha} f)(x) = f(x) - \sum_{i=1}^{n} \left[D_{a^+}^{\alpha-i} f(x)\big|_{x=a} \cdot \frac{(x-a)^{\alpha-i}}{\Gamma(\alpha-i+1)} \right],$

(v) $D_{a^+}^{-\alpha}(D_{a^+}^{\beta} f)(x) = D_{a^+}^{\beta-\alpha} f(x) - \sum_{i=1}^{n} \left[D_{a^+}^{\beta-i} f(x)\big|_{x=a} \cdot \frac{(x-a)^{\alpha-i}}{\Gamma(\alpha-i+1)} \right],$

(vi) $D_{a^+}^{\alpha}(D_{a^+}^{n} f)(x) = D_{a^+}^{\alpha+n} f(x) - \sum_{i=0}^{n-1} f^{(i)}(a) \cdot \frac{(x-a)^{i-\alpha-n}}{\Gamma(i-\alpha-n+1)},$

(vii) $D_{a^+}^{\alpha}(D_{a^+}^{\beta} f)(x) = D_{a^+}^{\alpha+\beta} f(x) - \sum_{i=1}^{n} \left[D_{a^+}^{\beta-i} f(x)\big|_{x=a} \cdot \frac{(x-a)^{-\alpha-i}}{\Gamma(1-\alpha-i)} \right].$

The detailed proofs of these identities can be found in [9], [18], and [1].

1.1.1.3 Laplace Transform of Riemann–Liouville Fractional Derivative

The general formula for the Laplace transform of the n-th derivative of a function is defined by [1]:

$$\mathcal{L}\left\{f^{(n)}(x)\right\}(s) = s^n \mathcal{L}\left\{f(x)\right\}(s) - \sum_{k=0}^{n-1} s^{n-k-1} f^{(k)}(0). \tag{1.10}$$

- The Laplace transform of the Riemann–Liouville fractional integral is simple and clear [9]. We have:

$$I^{\alpha} f(x) = \frac{1}{\Gamma(\alpha)} \int_0^x (x-\xi)^{\alpha-1} f(\xi)\, d\xi = \frac{1}{\Gamma(\alpha)} x^{\alpha-1} * f(x), \tag{1.11}$$

  where $*$ denotes the convolution operator.

  Applying the Laplace transform to the convolution of $\frac{1}{\Gamma(\alpha)} x^{\alpha-1}$ and $f(x)$, we obtain:

$$\mathcal{L}\left\{I^{\alpha} f(x)\right\}(s) = \frac{1}{s^{\alpha}} \mathcal{L}\left\{f(x)\right\}(s). \tag{1.12}$$

- The Laplace transform of the Riemann–Liouville fractional derivative is given by:

$$\mathcal{L}\left\{D^{\alpha} f(x)\right\}(s) = s^{\alpha} \mathcal{L}\left\{f(x)\right\}(s) - \sum_{k=0}^{n-1} s^{k} \left(D^{\alpha-k-1} f(x)\big|_{x=0} \right), \tag{1.13}$$

  where $n-1 < \alpha < n$.

  This formula is derived by applying the Laplace transform to the expression of the Riemann–Liouville derivative:

$$D^{\alpha} f(x) = \frac{d^n}{dx^n} \left(I^{n-\alpha} f(x) \right),$$

  and using the result from equation (1.12) followed by the classical derivative rule (1.10).

1.1.2 Caputo Fractional Derivatives

1.1.2.1 Definition and Basic Properties

Definition 1.1.3 *The fractional derivative of a function f(x) in the Caputo sense, is defined as follows, assuming that f(x) has n continuous and bounded derivatives:*

$$
\begin{aligned}
{}^{C}D^{\alpha}_{a+}f(x) &= (I^{n-\alpha}_{a} f^{(n)}(x)) = \frac{1}{\Gamma(n-\alpha)} \int_{a}^{x} (x-t)^{n-\alpha-1} f^{(n)}(t)\, dt, \\
&\qquad \textit{(the left-sided Caputo fractional Derivative).} \qquad \alpha \in [n-1, n[. \\
{}^{C}D^{\alpha}_{b-}f(x) &= (-1)^n (I^{n-\alpha}_{b} f^{(n)}(x)) = \frac{(-1)^n}{\Gamma(n-\alpha)} \int_{x}^{b} (t-x)^{n-\alpha-1} f^{(n)}(t)\, dt. \\
&\qquad \textit{(the right-sided Caputo fractional Derivative).}
\end{aligned}
\tag{1.14}
$$

Theorem 1.1.1 *(proof [9]) Let f be an absolutely continuous function with n-times differentiable on a given domain.*

$$
\begin{aligned}
D^{\alpha}_{a+}f(x) &= {}^{C}D^{\alpha}_{a+}f(x) + \sum_{j=0}^{n-1} \frac{(x-a)^{j-\alpha}}{\Gamma(j-\alpha+1)} f^{(j)}(a^{+}), \\
D^{\alpha}_{b-}f(x) &= {}^{C}D^{\alpha}_{b-}f(x) + \sum_{j=0}^{n-1} \frac{(-1)^j (b-x)^{j-\alpha}}{\Gamma(j-\alpha+1)} f^{(j)}(b^{-}).
\end{aligned}
$$

Property 1.1.3 *Let $\alpha, \beta \in \mathbb{R}^{+}$ with $\alpha \geq \beta$, and let $f \in C^{n+1}$ be a sufficiently smooth function. Then, the following properties hold:*

i) ${}^{C}D^{\alpha}_{a} I^{\alpha}_{a} f(x) = f(x)$.

ii) $\lim\limits_{\alpha \to n^{-}} {}^{C}D^{\alpha}_{a} f(x) = f^{(n)}(x)$.

iii) ${}^{C}D^{\alpha}_{a} f(x) = D^{\alpha}_{a} f(x)$ *if and only if* $D^{j} f(a) = 0 \quad \forall j \in \{0, 1, \ldots, n-1\}$.

iv) $I^{\alpha}_{a}\, {}^{C}D^{\alpha}_{a} f(x) = f(x) + \sum\limits_{k=1}^{n-1} \frac{f^{(k)}(a)}{k!} (x-a)^{k}$.

The detailed proofs of these identities can be found in [1].

1.1.2.2 Laplace Transform of the Caputo Fractional Derivative

The Laplace transform of the Caputo fractional derivative is given by:

$$
\mathcal{L}\left\{{}^{C}D^{\alpha}_{x} f(x)\right\}(s) = s^{\alpha} \mathcal{L}\{f(x)\}(s) - \sum_{k=0}^{n-1} s^{\alpha-k-1} f^{(k)}(0), \quad n-1 < \alpha \leq n. \tag{1.15}
$$

proof 1.1.1 *Taking the Laplace transform of Caputo fractional derivative:*

$$\begin{aligned}
\mathcal{L}\left\{{}^{C}D_x^{\alpha} f(x)\right\}(s) &= \mathcal{L}\left\{\frac{1}{\Gamma(n-\alpha)}\int_0^x (x-t)^{n-\alpha-1} f^{(n)}(t)\,dt\right\} \\
&= \mathcal{L}\left\{\left(\frac{x^{n-\alpha-1}}{\Gamma(n-\alpha)}\right) * f^{(n)}(x)\right\} \quad \textit{(Definition of convolution)} \\
&= \mathcal{L}\left\{\frac{x^{n-\alpha-1}}{\Gamma(n-\alpha)}\right\} \cdot \mathcal{L}\left\{f^{(n)}(x)\right\} \quad \textit{(Convolution theorem)} \\
&= s^{\alpha-n} \cdot \left(s^n \mathcal{L}\{f(x)\} - \sum_{k=0}^{n-1} s^{n-k-1} f^{(k)}(0)\right) \\
&\textit{where } \mathcal{L}\left\{\frac{x^{n-\alpha-1}}{\Gamma(n-\alpha)}\right\} = s^{\alpha-n} \\
&\mathcal{L}\left\{{}^{C}D_x^{\alpha} f(x)\right\}(s) = s^{\alpha}\mathcal{L}\{f(x)\} - \sum_{k=0}^{n-1} s^{\alpha-k-1} f^{(k)}(0).
\end{aligned}$$

For a detailed proof, see [18].

1.1.3 Grünwald–Letnikov Fractional Derivatives and Integrals

The Grünwald-Letnikov fractional derivative is based on finite differences instead of integrals. It is used to compute fractional derivatives numerically, making it suitable for computational applications and discrete systems.

1.1.3.1 Definition and Basic Properties

Let $f(x)$ be a continuous function. The first-order derivative of $f(x)$ is defined according to the standard definition as:

$$\frac{d}{dx} f(x) = \lim_{h\to 0} \frac{f(x) - f(x-h)}{h} \tag{1.16}$$

We can construct higher order derivatives directly by higher order backward Difference of a function $f(x)$ of order $n \in \mathbb{N}_0$ of the form :

$$\frac{d^n}{dx^n} f(x) = \lim_{h\to 0} \frac{1}{h^n} \sum_{k=0}^{n} (-1)^k \binom{n}{k} f(x-kh), \tag{1.17}$$

To move from the classical derivative to the fractional derivative, we change the variable $n \in \mathbb{N}_0$ by the real or the complex number α where $\alpha > 0$ or $\Re(\alpha) > 0$.

$${}^{G}D_x^{\alpha} f(x) = \lim_{h\to 0} \frac{1}{h^{\alpha}} \sum_{k=0}^{\infty} (-1)^k \binom{\alpha}{k} f(x-kh), \quad \alpha > 0 \tag{1.18}$$

where

$$\binom{\alpha}{k} = \frac{\alpha(\alpha-1)(\alpha-2)\ldots(\alpha-k+1)}{k!}. \tag{1.19}$$

$$\begin{bmatrix}\alpha\\k\end{bmatrix} = \frac{\alpha(\alpha+1)(\alpha+2)\ldots(\alpha+k-1)}{k!}. \tag{1.20}$$

$$\binom{-\alpha}{k} = \frac{-\alpha(-\alpha-1)(-\alpha-2)\ldots(-\alpha-k+1)}{k!} = (-1)^k \begin{bmatrix}\alpha\\k\end{bmatrix}.(\text{ According to [14]}) \tag{1.21}$$

Thus, the Grünwald-Letnikov fractional derivative is defined by the following expression:

$${}_a^G D_x^{\alpha} f(x) = \lim_{h\to 0}\frac{1}{h^{\alpha}}\sum_{k=0}^{n}(-1)^k\binom{\alpha}{k} f(x-kh), \qquad \alpha\in\mathbb{R}_+. \tag{1.22}$$

In order to define the Grünwald-Letnikov integral, a negative (α) must be used over (1.18). We find the following:

$${}_a^G D_x^{-\alpha} f(x) = \lim_{h\to 0}\frac{1}{h^{\alpha}}\sum_{k=0}^{n}(-1)^k\binom{-\alpha}{k} f(x-kh). \tag{1.23}$$

So the expression for the integral Grünwald-Letnikov is:

$${}_a^G D_x^{-\alpha} f(x) = \lim_{h\to 0}\frac{1}{h^{\alpha}}\sum_{k=0}^{n}\begin{bmatrix}\alpha\\k\end{bmatrix} f(x-kh) = \frac{1}{\Gamma(\alpha)}\int_a^x (x-t)^{\alpha-1} f(t)\,dt. \tag{1.24}$$

If the function $f(x)$ has (m + 1) continuous derivative, then

$${}_a^G D_x^{-\alpha} f(x) = \sum_{k=0}^{m}\frac{f^{(k)}(t-a)^{\alpha+k}}{\Gamma(\alpha+k+1)} + \frac{1}{\Gamma(\alpha+k+1)}\int_a^x (x-t)^{\alpha+m} f^{(m+1)}\,dt, \tag{1.25}$$

and

$${}_a^G D_x^{\alpha} f(x) = \sum_{k=0}^{m}\frac{f^{(k)}(t-a)^{k-\alpha}}{\Gamma(k-\alpha+1)} + \frac{1}{\Gamma(k-\alpha+1)}\int_a^x (x-t)^{m-\alpha} f^{(m+1)}\,dt.(\text{ According to [14]}) \tag{1.26}$$

Remark 1.1.2 *The appearance of integration in the two equations(1.22,1.24) was a result of applying the Riemann sum*

$$\int_a^b f(x)\,dx = \lim_{n\to\infty}\sum_{k=0}^{n-1} f(x_k)\Delta x_k.$$

.

Property 1.1.4 *[18]For any* $\Re(\alpha)\in\mathbb{R}$, $\Re(\beta)<0$, *and* $n\in\mathbb{N}$

i) $\frac{d^n}{dx^n}({}^G D_x^{\alpha} f(x)) = {}^G D_x^{\alpha+n} f(x),$

ii) $^{G}D_x^{\alpha}(\frac{d^n}{dx^n}f(x)) = \frac{d^n}{dx^n}(^{G}D_x^{\alpha}f(x)) - \sum_{k=0}^{n-1}\frac{f^{(k)}(a)(t-a)^{k-\alpha-n}}{\Gamma(k-\alpha-n+1)}$,

iii) ${}_a^{G}D_x^{\alpha}({}_a^{G}D_x^{\beta}f(x)) = {}_a^{G}D_x^{\alpha+\beta}f(x))$.

1.1.3.2 Laplace Transform of the Grünwald-Letnikov Fractional Derivative

Suppose that f has a Laplace transform $\mathcal{L}\{f(s)\}$ and $a = 0$, we have for $0 \leq \alpha < 1$:

$$^{G}D_x^{\alpha}f(x) = \frac{f(0)x^{-\alpha}}{\Gamma(1-\alpha)} + \frac{1}{\Gamma(1-\alpha)}\int_0^x (x-t)^{-\alpha}f'(t)\,dt, \tag{1.27}$$

then

$$\mathcal{L}\{^{G}D_x^{\alpha}f(x); s\} = \frac{f(0)}{s^{1-\alpha}} + \frac{1}{s^{1-\alpha}}(s\mathcal{L}\{f(x)\} - f(0)) = s^{\alpha}\mathcal{L}\{f(x)\}. \tag{1.28}$$

For a detailed proof, see [5]

1.1.4 Comparison of Fractional Derivatives

Property	**Riemann-Liouville Derivative**	**Caputo Derivative**	**Grünwald Derivative**
Mathematical Definition	Based on historical integral.	Based on integer derivatives of functions.	Based on numerical approximation using finite differences.
Initial Conditions	Based on the behavior of the function over time.	Traditional initial conditions like $f(0)$.	Numerical initial conditions, may depend on the difference between values.
Applications	Theoretical in mathematics and fractional calculus.	Practical in physics and engineering (dynamic systems).	Numerical in simulations and solving fractional differential equations.
Complexity	More complex from a theoretical perspective.	More practical and suited for specific applications.	Simpler from a numerical perspective, but less accurate.

Table 1.1: Comparison of Riemann-Liouville, Caputo, and Grünwald Derivatives

1.2 Ordinary Fractional Differential Equations

1.2.1 Linear Fractional Differential Equations

Definition 1.2.1 *Linear fractional differential equations are equations in which the derivatives of the unknown function $y(x)$ are of fractional order, and the equation is linear with respect to* *these derivatives. The equation does not contain any nonlinear functions of the unknown or its derivatives. The general form of a linear fractional differential equation is :*

$$a_0 D^{\alpha} y(x) + a_1 D^{\alpha-1} y(x) + \cdots + a_n y(x) = f(x). \tag{1.29}$$

Where:

- D^{α} *represents the fractional derivative of order* α,
- $a_0, a_1, \ldots, a_n$ *Constants or Functions that Vary with Time,*
- $f(x)$ *is a given function.*

Remark 1.2.1 *The equation is considered **homogeneous** if the given function* $f(x) = 0$. *If* $f(x) \neq 0$, *then the equation is considered **non-homogeneous**.*

1.2.2 Nonlinear Fractional Differential Equations

Definition 1.2.2 *The nonlinear fractional differential equation is an equation that contains fractional derivatives of the unknown function and is nonlinear due to the presence of nonlinear functions of the unknown or its derivatives. The general form of the nonlinear fractional differential equation.*

$$a_0 D^{\alpha} y(x) + a_1 D^{\alpha-1} y(x) + \cdots + a_n y(x) + g(y(x), D^{\beta} y(x)) = f(x). \tag{1.30}$$

Where:

- $D^{\alpha} y(x)$ *represents the fractional derivative of order* α.
- $a_0, a_1, \ldots, a_n$ *are constants or functions that may vary with time.*
- $g(y(x), D^{\beta} y(x))$ *is a nonlinear function involving the unknown function* $y(x)$ *or its derivatives.*
- $f(x)$ *is a given function.*

Example 1.2.1

$$D^{\frac{3}{2}} y(x) + \frac{1}{2} D^{\frac{5}{2}} y(x) + \ln y(x) = 0. \tag{1.31}$$

This is a homogeneous nonlinear fractional differential equation because the logarithmic function is nonlinear, and the second term of the equation equals zero.

1.2.3 Cauchy Problem for Differential Equations of Fractional Order

Definition 1.2.3 *[9] The Cauchy problem is defined by an equation of fractional order and an initial condition as follows:*

$$(IPV) \quad \begin{cases} D_x^\alpha y = f(x,y), \quad \forall x \in [0,T], \quad \text{with} \quad n-1 < \alpha < n, n \in \mathbb{N} \\ (D_x^{\alpha-k} y)(0) = b_k, \qquad\qquad k = 1,\dots,n. \end{cases} \tag{1.32}$$

Where b_k are the initial values given at $x = 0$. The Riemann-Liouville derivative is undefined when $x = 0$, so the initial condition is written as follows:$(D_x^{\alpha-k} y)(0) = \lim_{x\to 0}(D_x^{\alpha-k} y)(x)$. The Caputo derivative does not have this drawback.

The Caputo derivative is the best choice when working with initial conditions because it is well defined when $x = 0$.

Lemma 1.2.1 ([10]) *Let $0 < \alpha < 1$, and let $f : [0,T] \to \mathbb{R}$ be a continuous function. A function y is a solution to the Cauchy problem*

$$\begin{cases} D_x^\alpha y(x) = f(x, y(x)), \quad \forall x \in [0,T], \\ (D_x^{\alpha-k} y)(0) = b_k, \qquad k = 1,\dots,n-1, \quad \text{where } n-1 < \alpha < n, \ n \in \mathbb{N}, \end{cases} \tag{1.33}$$

if and only if it is a solution to the Volterra integral equation

$$y(x) = \sum_{k=1}^{n} \frac{b_k x^{\alpha-k}}{\Gamma(\alpha-k+1)} + \frac{1}{\Gamma(\alpha)} \int_0^x (x-t)^{\alpha-1} f(t, y(t))\, dt. \tag{1.34}$$

In particular, when $0 < \alpha < 1$, the equation reduces to:

$$y(x) = b_0 + \frac{1}{\Gamma(\alpha)} \int_0^x (x-t)^{\alpha-1} f(t, y(t))\, dt. \tag{1.35}$$

1.2.4 Methods for Solving Ordinary Fractional Differential Equations:

1.2.4.1 Analytical Methods (Laplace Transform Method)

Solving fractional differential equations using the Laplace transform is an effective method for dealing with equations involving derivatives of fractional order. This approach relies on transforming the differential equation into an algebraic equation in the frequency domain using the Laplace transform, and then returning to the original domain using the inverse transform.

Example 1.2.2 *The equation we are working with is:*

$$D^{0.75} y(x) = 0, \quad y(0) = y_0. \tag{1.36}$$

We take the Laplace transform of both sides, using the Laplace transform of the Caputo derivative:

$$\mathcal{L}\{D^{0.75}y(x)\} = s^{0.75}\mathcal{L}\{y(x)\} - s^{-0.25}y(0).$$

The equation becomes:

$$\mathcal{L}\{y(x)\} = \frac{y(0)}{s^1}.$$

Now, we apply the inverse Laplace transform to get the solution in the time domain x (Based on the table in the annex).

$$y(x) = y(0).$$

Theorem 1.2.1 *(proof [10]) Let $n-1 < \alpha \leq n$ $(n \in \mathbb{N})$ and $\lambda \in \mathbb{R}$. Then the functions*

$$y_j(x) = x^{\alpha-j}E_{\alpha,\alpha+1-j}(\lambda x^\alpha) \quad (j = 1, 2, \ldots, n), \tag{1.37}$$

produce the fundamental system of solutions to the following equation:

$$\sum_{k=1}^{m} b_k \left(D_{0+}^{\alpha_k}y\right)(x) + b_0 y(x) = 0 \quad for \quad x > 0, \quad 0 < \alpha_1 <, \ldots, < \alpha_m, \quad n-1 < \alpha_m \leq n, \quad m, n \in \mathbb{N} \tag{1.38}$$

Example 1.2.3

$$D^{\frac{3}{2}}y(x) = 0. \tag{1.39}$$

we have $1 < \alpha = \dfrac{3}{2} \leq 2$ and $b = \lambda$, Thus, we need to calculate two solutions y_1 and y_2.

$$y_1 = x^{\frac{1}{2}}E_{\frac{3}{2},\frac{3}{2}}(bx^{\frac{3}{2}}), \quad for j = 1. \tag{1.40}$$

$$y_2 = x^{-\frac{1}{2}}E_{\frac{3}{2},\frac{1}{2}}(bx^{\frac{3}{2}}), \quad for j = 2. \tag{1.41}$$

1.2.4.2 Numerical Methods (Finite Difference Method)

The finite difference method is a numerical technique used to solve fractional or classical differential equations. It transforms the differential equations into a system of algebraic equations, where the derivatives are replaced by finite differences (i.e., the differences between the function values at adjacent points in time or space).

- **Types of Finite Differences:**
  We use the first two terms of the Taylor series at the point $x_j + h$, near the point x_j, to obtain the forward difference, which is defined as:

$$y'(x_j) \approx \frac{y(x_j + h) - y(x_j)}{h}. \tag{1.42}$$

By replacing h with $-h$, we obtain the backward difference:

$$y'(x_j) \approx \frac{y(x_j) - y(x_j - h)}{h}. \tag{1.43}$$

The third type is the central difference, which is usually more accurate than the forward or backward differences. It is obtained by adding equations (1.42) and (1.43) and is defined as:

$$y'(x_j) \approx \frac{y(x_j + h) - y(x_j - h)}{2h}. \tag{1.44}$$

- **Solution Steps:**
  - **Discretization of the domain:** The continuous domain is divided into a grid or mesh.
  - **Approximation of the fractional derivatives:** Use Grünwald-Letnikov or Caputo definitions to approximate the fractional derivatives.
  - **Solving the system of equations:** Solve the resulting algebraic system using numerical solvers such as Gaussian elimination or LU decomposition.

Example 1.2.4 *Solve the homogeneous fractional differential equation:*

$$D^{\frac{7}{2}} y(x) + py(x) = 0, \qquad \textit{where } p \textit{ is a constant.} \tag{1.45}$$

with initial conditions: $y(0) = 1$, $y'(0) = 0$.

- ***Discretizing the domain:***
  We divide the domain $[0, L]$ *into* N *points, where:*

$$L = 1, \quad N = 10, \quad 0 \leq x \leq 1,$$

$$x_n = nh, \quad x_{n-k} = (n-k)h, \quad \textit{where} \quad h = \frac{L}{N} = 0.1$$

  Thus, we obtain the points:

$$x_0, x_1, x_2, \ldots, x_{10}.$$

- ***Approximating the fractional derivative using finite differences:***
  We use the Grünwald-Letnikov approximation for the fractional derivative, given by:

$$D_x^{\frac{7}{2}} y(x_n) \approx \frac{1}{h^{7/2}} \sum_{k=0}^{n} (-1)^k \binom{7/2}{k} y(x_n - kh).$$

  We denote the Grünwald weights by w_k, *where:*

$$w_k = (-1)^k \binom{7/2}{k} = (-1)^k \frac{\Gamma(9/2)}{\Gamma(k+1)\Gamma(9/2 - k)}. \tag{1.46}$$

We compute the Grünwald weights:

$$w_0, w_1, w_2, w_3, \ldots$$

Substituting equation (1.46) into the fractional differential equation, we get:

$$y_n = -\frac{1}{ph^{7/2}} \sum_{k=1}^{n} w_k y_{n-k}. \tag{1.47}$$

Based on the recurrence formula (1.47), we compute the values of y_n from x_0 to x_{10}. We can solve the resulting system using numerical methods such as Gaussian elimination or LU decomposition to find the values of $y_1, y_2, \ldots, y_{10}$.

1.3 Fractional Partial Differential Equations

A general fractional partial differential equation can be represented as:

$$D_t^{\alpha} u(x,t) = L(u(x,t)), \tag{1.48}$$

where:

- D_t^{α} is the fractional derivative with respect to time of order α.
- $L(x,t)$ is a differential operator.

1.3.1 Examples of Fractional Partial Differential Equations

Many well known fractional partial differential equations exist, such as the fractional diffusion equation, fractional wave equation, heat equation, fractional Laplace equation, and others. Below, we present two examples.

- **Fractional Diffusion Equation**
  The general form of a fractional diffusion equation is:

$$D_t^{\alpha} u(x,t) = k D_x^{\beta} u(x,t). \tag{1.49}$$

  where:

  - D_t^{α} is the fractional derivative in time t of order α, with $0 < \alpha \leq 1$.
  - D_x^{β} is the fractional derivative in space x of order β, with $0 < \beta \leq 2$.
  - k is a constant that relates the space and time derivatives, often interpreted as a diffusion coefficient.

It is used to model non-traditional diffusion processes[10], such as diffusion in heterogeneous media, like water flow in rocks or molecule transport in biological tissues.

- **Fractional Wave Equation**
  In fractional wave equations, fractional temporal or spatial derivatives are used. The general form is written as follows:

$$D_t^\alpha u(x,t) = c^2 D_x^\beta u(x,t), \quad 0 < \alpha, \beta \leq 2 \qquad 0 < x < l, \quad t > 0 \tag{1.50}$$

  where:

  - $D_t^\alpha u(x,t)$ is the fractional temporal derivative of order α.
  - $D_x^\beta u(x,t)$ is the fractional spatial derivative of order β.
  - c is the speed of the wave.

  Fractional wave equations are used in many fields that require modeling waves in non-traditional media, such as dispersive media, systems with memory[10], and waves in biological tissues.

1.3.2 Initial and Boundary Conditions

- **Initial Condition** The initial condition specifies the state of the system at time $t = 0$. It is typically given as:

$$u(x,0) = f(x), \quad 0 \leq x \leq l. \tag{1.51}$$

- **Boundary Conditions** Boundary conditions control the values that the solution must satisfy at the spatial domain boundaries. There are different types of boundary conditions:

  - **Dirichlet Condition** Specifies the **value** of u at the boundaries:

$$u(0,t) = 0, \quad u(l,t) = 0.$$

  - **Neumann Condition** Specifies the **derivative** of u at the boundaries:

$$\left.\frac{\partial u}{\partial x}\right|_{x=0} = 0.$$

  - **Robin Condition** A combination of Dirichlet and Neumann conditions:

$$au + b\frac{\partial u}{\partial x} = g(t).$$

These conditions play a crucial role in solving partial differential equations, ensuring well-posedness and uniqueness of solutions.

the fractional partial differential equations can be solved using several of the same methods mentioned earlier for solving fractional-order differential equations. These methods include the Laplace transform and Fourier transform, as well as solutions using the Mittag-Leffler function in analytical approaches. Additionally, numerical solutions can be obtained using the finite difference method. (For exploring the solution methods [1]).

CHAPTER 2

FRACTIONAL BIOMEDICAL MODELS

2.1 Overview of Mathematical Modeling

Mathematical modeling is the process of representing a real-world phenomenon, influenced by various factors, into a mathematical relationship. It is a fundamental tool used in a wide range of fields (such as physics, engineering, and biology). This representation is usually expressed through equations or functions. Mathematical modeling helps simplify complex systems, making it easier to understand and analyze their behavior, predict their results, and optimize their performance using available information. Modeling follows a systematic process that involves organized steps [13][17], beginning with the following:

- **Identifying and understanding the real-world Phenomenon.**
- **Selecting important factors and variables, and excluding less relevant details.**
- **Formulating mathematical equations:**
  - Differential Equations: If the system is dynamic and time-dependent.
  - Algebraic Equations: If the system is static.
  - Probabilistic Equations: If there is uncertainty or randomness in the phenomenon.
- **Finding analytical or numerical solutions**
- **Validating the model by comparing its results with real data or scientific experiments.**
- **Using the model for prediction or analyzing the impact of varying factors.**

Example 2.1.1 *Simple Mathematical Modeling of a Physical Phenomenon – Ohm's Law*

$$V = I \cdot R.$$

Variables:

- V*: Voltage (in volts).*
- I*: Electric current (in amperes).*
- R*: Resistance (in ohms).*

This model represents a simple linear relationship between the three variables. It can be used to predict the behavior of the electrical system under certain conditions.

Mathematical modeling is an important tool in many sciences, including biomedical science, as it helps in studying biomedical processes more accurately and understanding the interactions between different factors in the biomedical system. Mathematical modeling in biomedical initially relied on ordinary differential equations (ODEs). However, as science advanced, the limitations of classical ODEs which assume local and memory less dynamics became apparent for complex biomedical systems. Many phenomena, such as drug diffusion or tumor growth often exhibit delayed responses, or non-homogeneous temporal behaviors. Fractional calculus addresses these challenges by introducing non-integer derivatives, enabling more accurate modeling of memory effects and non-local interactions

Among these models that have evolved in biomedical, we can mention:

- The disease spread model.
- The blood flow model within blood vessels.
- The tissue and cancer tumor growth model.

In this thesis, we will focus on the following two models:

- Drug diffusion model across the skin.
- A Predator–Prey Model with Infectious Disease in the Prey Population.

2.2 Drug Diffusion Model Across the Skin

2.2.1 Biological Overview

Transdermal drug delivery is an advanced technique that offers an effective and safe alternative to traditional methods such as oral pills and injections. This method relies on the gradual absorption of the drug through the skin until it reaches the bloodstream, helping to maintain a stable drug concentration and reduce side effects.

However, the penetration of drugs through human skin is a complex and intricate process due to multiple layers that act as barriers to drug entry. The first barrier is the stratum corneum, the outermost layer composed of dead cells surrounded by a lipid matrix, making it a strong barrier that prevents most drugs from passing through, especially hydrophilic ones. Beneath it lies the epidermis, a living layer without blood vessels that plays a role in regulating the passage of drug compounds, particularly lipophilic ones. Finally, the dermis is the deepest layer, containing blood vessels responsible for drug absorption and transport into systemic circulation [7].

This technique is used to deliver a variety of drugs, such as nicotine patches to aid in smoking cessation and morphine patches for chronic pain relief. The success of transdermal drug absorption depends on the drug's physicochemical properties, such as its lipid solubility and molecular size, as well as the interaction of its components with the different skin layers [15].

See Fig 2.1, which illustrates the main structural components of human skin [4].

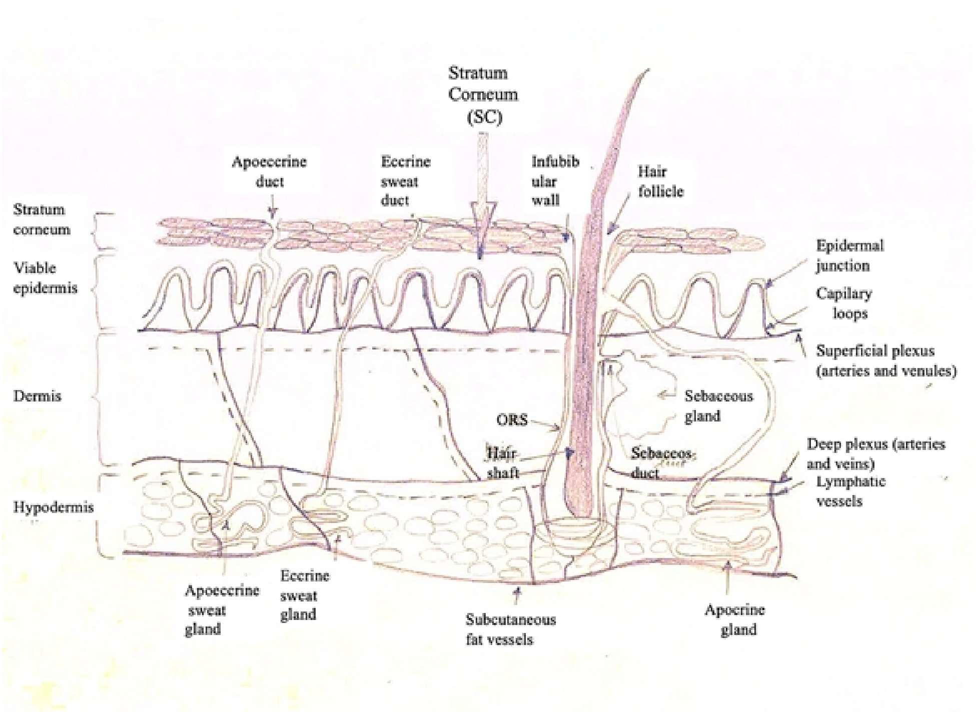

Figure 2.1: Illustration of the layers of human skin

2.2.2 The Classical Model

The classical model of drug diffusion through the skin can be mathematically represented using Fick's second law [4], which is expressed as follows:

$$\frac{\partial c(x,t)}{\partial t} = D\frac{\partial^2 c(x,t)}{\partial x^2}, \tag{2.1}$$

where:

- $c(x,t)$ is the concentration of the drug at position x and time t.
- D is the constant diffusion coefficient.
- x is the distance across the skin layers.

This model assumes linear diffusion without considering memory effects or nonlinear influences. The model is expressed in Figure 2.2, where the skin is considered as a homogeneous layer with a thickness h, located between the donor and the receiver, and it satisfies the following conditions:

$$c(0,t) = c_0, \quad c(h,t) = 0, \quad \forall t \in \mathbb{R}_+^*. \qquad \text{(boundary conditions.)} \tag{2.2}$$

$$c(x,0) = 0, \quad \text{for} \quad 0 \leq x \leq h. \qquad \text{(initial condition.)} \tag{2.3}$$

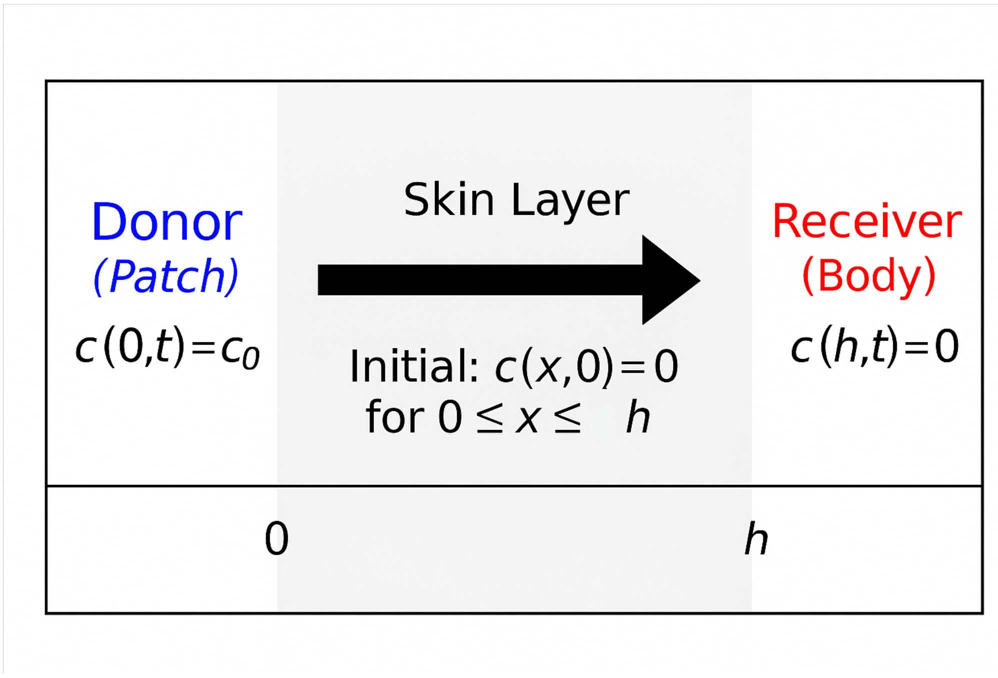

Figure 2.2: Drug transport in a homogeneous skin layer: schematic view

We solve the classical model (2.1) using the method of separation of variables [3] to obtain the following concentration expression:

$$c(x,t) = c_0 \left(1 - \frac{x}{h} - \frac{2}{\pi} \sum_{n=1}^{\infty} \frac{1}{n} \sin\left(\frac{n\pi x}{h}\right) \exp\left(-\frac{n^2\pi^2 t}{t_d}\right)\right), \tag{2.4}$$

where $t_d = \dfrac{h^2}{D}$ is the characteristic time of diffusion.
The drug concentration obtained by solving the model contributes to determining the drug flux value $j(t)$ and the total dissolved quantity $q(t)$, based on Fick's first law, as shown in the following equations:

$$j(t) = -D \frac{\partial c(x,t)}{\partial x}\bigg|_{x=h} = Dc_0 \left(\frac{1}{h} - \frac{2\pi}{h^2} \sum_{n=1}^{\infty} (-1)^n \exp\left(-\frac{n^2\pi^2 t}{t_d}\right)\right). \tag{2.5}$$

$$q(t) = A \int_0^t j(s)ds = Ac_0 h \left(\frac{t}{t_d} - \frac{1}{6} - \frac{2}{\pi^2} \sum_{n=1}^{\infty} \frac{1}{n^2} \exp\left(-\frac{n^2\pi^2 t}{t_d}\right)\right). \tag{2.6}$$

Where, A is the area across the section of the layer through which the drug is transferred.
The equations are transformed into the Laplace domain to simplify the complex differential equations involving time.

$$C(x,s) = \mathcal{L}[c(x,t)], \quad J(x,s) = \mathcal{L}[j(x,t)], \quad Q(x,s) = \mathcal{L}[q(x,t)].$$

$$C(x,s) = \frac{c_0 \sinh\left(\sqrt{st_d}\left(1 - \frac{x}{h}\right)\right)}{s \sinh\left(\sqrt{st_d}\right)}.$$

From this solution, the flux $J(x,s)$ and the total quantity of solute $Q(x,s)$ [3], can be expressed as :

$$J(x,s) = D \frac{\partial C(x,s)}{\partial x}\bigg|_{x=h} = D \frac{c_0 \sqrt{st_d}}{sh \sinh \sqrt{st_d}}.$$

$$Q(x,s) = \frac{AJ(x,s)}{s} = \frac{ADc_0}{s^2 h} \sqrt{\frac{st_d}{p}} \sinh\left(\sqrt{\frac{st_d}{p}}\right).$$

This transformation facilitates numerical handling and improves the accuracy of the results when calculating the drug flux and the total amount of drug, in order to avoid the accumulation of errors.

This model provides a good starting point for understanding the general principles of drug transport through the skin. It is one of the simplest mathematical models used to study drug diffusion across the skin. However, this model is an oversimplification as it does not consider the skin's multilayered structure. To overcome the limitations imposed by this model, the skin can be considered as a multilayered structure, where it is divided into three main layers: the stratum corneum, the epidermis, and the dermis. A specific diffusion coefficient (D_i) and partition coefficient (k_i) are assigned to each layer, allowing for a more accurate description of the transport process across the skin. The flux across each layer can be expressed as:

$$J_i = -D_i \frac{\partial c}{\partial x},$$

where:

- J_i is the flux in the i-th layer.
- D_i is the diffusion coefficient for that layer.
- $\frac{\partial c}{\partial x}$ is the concentration gradient in the layer.

For a more detailed description of the latter model [3].

2.2.3 The Fractional-Order Model

Although the classical model that divides the skin into layers represents an improvement over the initial model, it still relies on linear assumptions that may be insufficient in certain cases. In such situations, fractional models based on fractional differential equations (as discussed in Chapter One) can be used to describe drug transport through the skin, Because they take into account nonlinear phenomena and complex interactions between drug molecules and skin tissues.

We assume the presence of a homogeneous layer with thickness h, through which the drug spreads with concentration $c(x,t)$, which varies with time t and spatial location $x \in [0,h]$. The traditional time derivative is replaced by the Caputo fractional derivative of order $\alpha \in (0,1)$ [4], yielding the following fractional diffusion equation:

$$ {}^{C}\mathcal{D}_t^{\alpha} c(x,t) = D \frac{\partial^2 c(x,t)}{\partial x^2}, \quad 0 < x < h, \quad t > 0, \tag{2.7}$$

where:

- ${}^{C}\mathcal{D}_t^{\alpha}$ the Caputo fractional derivative of order α.
- D is the diffusion coefficient.
- $c(x,t)$ is the concentration of the drug at position x and time t.

The same initial and boundary conditions as in the classical model (see Eqs (2.1), (2.2), and (2.3)) are applied to complete the fractional model.

To solve the model represented by the fractional differential equations, we will use one of the methods discussed in Chapter 1. In this case, the Laplace transform will be employed, as it is considered one of the powerful analytical tools for solving complex fractional diffusion equations.
We apply the Laplace transform to the equation (2.7), using the standard property of the Caputo fractional derivative (1.15):

$$\mathcal{L}\left\{{}^{C}\mathcal{D}_t^{\alpha}c(x,t)\right\} = s^{\alpha}\mathcal{L}\{c(x,t)\} - s^{\alpha-1}c(x,0). \tag{2.8}$$

Since the initial condition is $c(x,0)=0$, the equation becomes:

$$s^{\alpha}\mathcal{L}\{c(x,t)\} = D\frac{\partial^2\mathcal{L}\{c(x,t)\}}{\partial x^2}. \tag{2.9}$$

This is a second-order linear homogeneous differential equation with constant coefficients:

$$\frac{\partial^2\mathcal{L}\{c(x,t)\}}{\partial x^2} - \frac{s^{\alpha}}{D}\mathcal{L}\{c(x,t)\} = 0. \tag{2.10}$$

The general solution is of the form:

$$\mathcal{L}\{c(x,t)\} = A(s)e^{\lambda x} + B(s)e^{-\lambda x}, \tag{2.11}$$

where $\lambda = \sqrt{\dfrac{s^{\alpha}}{D}}$. At $x=0$, we have:

$$\mathcal{L}\{c(0,t)\} = \frac{c_0}{s} \quad \Rightarrow \quad B(s) + A(s) = \frac{c_0}{s}. \tag{2.12}$$

At $x=h$, the condition is:

$$\mathcal{L}\{c(h,t)\} = 0 \quad \Rightarrow \quad A(s)e^{\lambda h} + B(s)e^{-\lambda h} = 0. \tag{2.13}$$

From this, we deduce:

$$A(s) = -B(s)e^{-2\lambda h}. \tag{2.14}$$

By substituting A(s) and B(s) and simplifies, we get:

$$\mathcal{L}\{c(x,t)\} = B(s)\left(e^{\lambda(x-h)} - e^{-\lambda(x+h)}\right).$$

The hyperbolic sine function $\sinh(x)$ can be expressed in terms of the exponential function as follows:

$$\sinh(x) = \frac{e^{x}-e^{-x}}{2}. \tag{2.15}$$

Therefore, the solution becomes:

$$\mathcal{L}\{c(x,t)\} = \frac{c_0}{s} \cdot \frac{\sinh\left(\sqrt{\frac{s^\alpha}{D}}(h-x)\right)}{\sinh\left(\sqrt{\frac{s^\alpha}{D}}h\right)}. \tag{2.16}$$

The inverse Laplace transform of this expression leads to an exact solution in the time domain, which resembles the classical solution but replaces the exponential function with the Mittag-Leffler function [4]:

$$c(x,t) = c_0\left(1 - \frac{x}{h}\right) - \frac{2c_0}{\pi}\sum_{n=1}^{\infty}\frac{1}{n}\sin\left(\frac{n\pi x}{h}\right)E_\alpha\left(-\frac{n^2\pi^2 D}{h^2}t^\alpha\right). \tag{2.17}$$

This solution generalizes the classical diffusion result (recovered when $\alpha = 1$), and captures memory effects and anomalous transport behavior observed in complex or biological media.

2.2.4 Comparison between the classical model and the fractional model

- **Memory Property and Lag Time Representation**

  Classical: Does not account for past temporal effects and requires the explicit inclusion of lag time.

  Fractional: Incorporates the memory property, where the current state depends on the entire past history, and the lag time emerges naturally [7].

- **Diffusion Pattern**

  Classical: Describes normal (Gaussian) diffusion, where the spreading distance increases with the square root of time.

  Fractional: Describes anomalous (non-Gaussian) diffusion, often exhibiting subdiffusive behavior that can generate non-Gaussian curves accurately reflecting the experimental behavior of the drug [3] [4].

- **Accuracy of Biological Representation**

  Classical: Assumes ideal and instantaneous diffusion behavior, which may not accurately reflect the complex physiological reality.

  Fractional: Represents the non instantaneous interactions between the drug and skin tissues [15], capturing the complex temporal nature of absorption.

2.3 A Predator–Prey Model with Infectious Disease in the Prey Population

2.3.1 Biological Overview

The predator-prey relationship is one of the most extensively studied biological interactions. When an element of epidemic infection is introduced into this relationship particularly among members of the prey population the population dynamics become more complex. When prey are infected with a contagious disease, the population typically splits into two categories: healthy (susceptible) prey and infected prey. It is often assumed that transmission occurs through direct contact or via the environment. This change in the composition of the prey population is reflected in:

1.Prey Population

- **Decrease in Prey Population:** The spread of a lethal disease among prey can lead to a rapid decline in their numbers.
- **Behavioral Changes:** Some diseases weaken the prey or slow their movement, making them easier to catch.
- **Natural Selection:** Over time, only prey with stronger immune resistance may survive, leading to changes in the genetic makeup of the population.

2.Predators Population

- **Food Scarcity:** The decline in prey populations due to disease may result in starvation among predators, or force them to switch to alternative prey species.
- **Risk of Infection Transmission:** Some diseases can be transmitted from prey to predators, posing a health threat to the predators .
- **Change in Hunting Strategy:** Predators may prefer to hunt infected prey due to ease of capture.

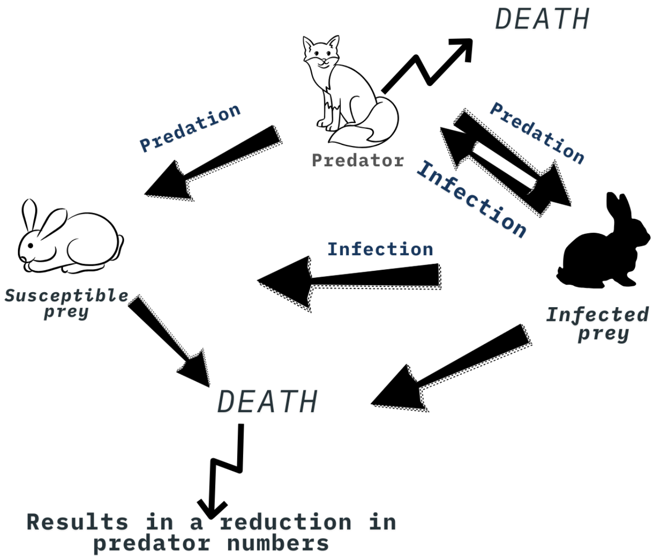

Figure 2.3: A simplified model of predator–prey interaction with disease

2.3.2 The Classical Model

To formulate the classical model (using classical differential equations), the following assumptions [6] must be considered:

- The prey is divided into two categories: infected prey $I(t)$ and healthy prey $S(t)$ become infected upon contact with infected prey.
- The healthy prey grows according to a logistic model characterized by an intrinsic growth rate r and an environmental carrying capacity k, which represents the maximum population size that the environment can sustain.
- The infected prey die due to the disease (their recovery is not taken into account).
- The predators $Y(t)$ do not rely entirely on these prey.
- All prey, both susceptible and infected, serve as food for the predators, but it is easier for the predators to catch the infected prey.

Based on the previous assumptions, we formulate the following model [6]:

$$\begin{cases} \dfrac{dS}{dt} &= r_1 S\left(1-\dfrac{S+I}{k_1}\right)-\lambda SI-\dfrac{p_1S^2Y}{1+S+\theta I}, \\ \dfrac{dI}{dt} &= \lambda SI-\dfrac{p_2I^2Y}{1+S+\theta I}-\gamma I, \\ \dfrac{dY}{dt} &= r_2Y\left(1-\dfrac{Y}{k_2+S+mI}\right)+\sigma_1\left(\dfrac{p_1S^2Y}{1+S+\theta I}\right)-\sigma_2\left(\dfrac{p_2I^2Y}{1+S+\theta I}\right), \end{cases} \tag{2.18}$$

$$S(0)\geq 0, \quad I(0)\geq 0, \quad Y(0)\geq 0. \quad (initial \quad conditions) \tag{2.19}$$

where

- r_1, r_2: Per capita growth rate of the prey and predators,respectively.
- k_1, k_2:The maximum capacity of the environment to support the number of prey and predators,respectively.
- p_1, p_2: Maximum rates of consumption of susceptible and infected prey,respectively.
- θ: Predator's rate of preference for the infected.
- λ : The rate of infection spread from infected prey to susceptible prey.
- γ: Per capita mortality rate of infected prey due to the disease.
- m : The rate of the environment's ability to support predators due to their consumption of infected prey.
- σ_1, σ_2 : The rate of predator's response to the type of prey consumed (infected or healthy).

Interpretation of the Model Terms

1- Equation of the Healthy Prey (S)

$$\frac{dS}{dt} = \underbrace{r_1 S \left(1 - \frac{S+I}{k_1}\right)}_{\text{Logistic growth of S}} - \underbrace{\lambda SI}_{\text{Infection transmission}} - \underbrace{\frac{p_1 S^2 Y}{1+S+\theta I}}_{\text{Y-to-S predation rate}} . \tag{2.20}$$

2- Equation of the Infected Prey (I)

$$\frac{dI}{dt} = \underbrace{\lambda SI}_{\text{Infection transmission}} - \underbrace{\frac{p_2 I^2 Y}{1+S+\theta I}}_{\text{Y-to-I predation rate}} - \underbrace{\gamma I}_{\text{Infected prey mortality}} . \tag{2.21}$$

3- Equation of the Predators (Y)

$$\frac{dY}{dt} = \underbrace{r_2 Y \left(1 - \frac{Y}{k_2+S+mI}\right)}_{\text{Logistic growth of Y}} + \underbrace{\sigma_1 \left(\frac{p_1 S^2 Y}{1+S+\theta I}\right)}_{\text{The positive effects of predation on S}} - \underbrace{\sigma_2 \left(\frac{p_2 I^2 Y}{1+S+\theta I}\right)}_{\text{The negative effects of predation on I}} . \tag{2.22}$$

Existence and Uniqueness of the Solution

To establish the existence and uniqueness of a solution to the system of differential equations (2.18) with the initial conditions (2.19), we invoke the classical Picard–Lindelöf theorem. This theorem requires the following two conditions to be satisfied:

- **Continuity of the right-hand side functions**: The functions $\frac{dS}{dt}$, $\frac{dI}{dt}$, and $\frac{dY}{dt}$ are continuous in their domain. Since all expressions are composed of polynomials and rational functions with non-zero denominators in the biologically meaningful domain, continuity is ensured.

- **Lipschitz continuity in the state variables S, I, and Y**: The partial derivatives of the right-hand side functions with respect to S, I, and Y are bounded in any closed and bounded subset of the domain

$$\mathcal{D} = \{(S, I, Y) \in \mathbb{R}^3 \mid S \geq 0,\ I \geq 0,\ Y \geq 0\},$$

which is the biologically relevant region.

Therefore, by the Picard–Lindelöf theorem, the system (2.18) admits a unique local solution in a neighborhood of the initial time within the domain $\mathcal{D}$.
Reference [16] provides a detailed analysis of the existence and uniqueness proof for an equivalent model.

The tight nonlinear coupling of variables in the system impedes analytical tractability, as the equations cannot be decoupled. The presence of multiplicative interaction terms (e.g.SI, I^2Y) renders explicit solutions infeasible, necessitating numerical, which are presented in Chapter 3.

2.3.3 The Fractional-Order Model

Traditional computation is less effective in describing complex environmental phenomena. Note that all the models mentioned above are in the form of a system of first-order differential equations, meaning that the growth rate of each population group depends only on the current state. In reality, the growth rate also depends on all past states (known as memory effects). To incorporate such effects, researchers apply a system of fractional differential equations [16], where the order of the derivative indicates the memory rate, as follows:

$$\begin{cases} {}^{C}D_t^{\alpha} S(t) &= r_1^{\alpha} S \left(1 - \dfrac{S+I}{k_1}\right) - \lambda^{\alpha} SI - \dfrac{p_1^{\alpha} S^2 Y}{1+S+\theta I}, \\ {}^{C}D_t^{\alpha} I(t) &= \lambda^{\alpha} SI - \dfrac{p_2^{\alpha} I^2 Y}{1+S+\theta I} - \gamma^{\alpha} I, \\ {}^{C}D_t^{\alpha} Y(t) &= r_2^{\alpha} Y \left(1 - \dfrac{Y}{k_2+S+mI}\right) + \sigma_1 \dfrac{p_1^{\alpha} S^2 Y}{1+S+\theta I} - \sigma_2 \dfrac{p_2^{\alpha} I^2 Y}{1+S+\theta I}. \end{cases} \tag{2.23}$$

where $\alpha \in [0, 1]$.

Since time is associated with the order of the fractional derivative α , it is necessary to adjust all time dependent parameters to be consistent with this change. To maintain dimensional consistency in the equations, the time dependent parameters are rescaled by raising them to the power of α.

To study the existence and uniqueness of the system (2.23), we define the region $\Omega \times [0, T]$, where

$$\Omega = \left\{ (S, I, Y) \in \mathbb{R}^3 \;\middle|\; \max\{|S|, |I|, |Y|\} \leq M \right\}, \quad T < \infty,$$

and M is sufficiently large.

Theorem 2.3.1 *For each $X_0 = (S_0 I_0 Y_0) \in \Omega$, there exist sa unique solution X(t) of the Caputo fractional differential system (2.23) with the initial condition $X_0 \in \Omega$, which is defined for all $t \geq 0$.*

Detailed proof in the reference [11].

2.3.4 Comparison between the classical model and the fractional model

- **Infection transmission**: The classical model uses a simple term to represent infection transmission, namely λSI, and assumes instantaneous and homogeneous interaction between individuals. This representation does not account for factors such as exposure duration or the evolution of immune response [6]. In contrast, fractional models allow for the representation of this time dependent cumulative behavior.

- **Time delay**: When a healthy prey comes into contact with an infected one, transmission does not necessarily occur immediately there may be an incubation period before symptoms appear. Similarly, a predator does not benefit directly from consuming prey; rather, the effects on its survival and reproduction manifest after a delay. This time delay is challenging to represent in classical models [2], whereas the fractional model automatically captures it through the structure of its derivatives.

- **Complex predator-prey interactions**: The classical model cannot represent the gradual shift from preying on healthy prey to targeting infected prey (due to their weakened state and easier capture). In contrast, fractional models are inherently suited to this transition.

- **Disease-induced mortality rate** : The classical model assumes that the mortality rate of infected prey is represented by a constant term γI, applied instantaneously and uniformly to all infected individuals [11]. In contrast, the fractional-order model accounts for the duration of infection and is capable of incorporating the cumulative effect of the infection period into the system dynamics.

CHAPTER 3

APPLICATIONS

To compare the behavior of the classical and fractional-order models discussed in the previous chapter and verify the flexibility of fractional models in representing complex biomedical phenomena, we conduct numerical simulations using the finite difference method for both classical and fractional models.

3.1 First Model (Diffusion of 4-Cyanophenol through Human Skin)

To evaluate the accuracy of fractional order models compared to classical models of transdermal drug diffusion, we rely on experimental data reported by Pirot et al (1997).

3.1.1 Experiment

A saturated aqueous solution of 4-cyanophenol was applied onto a patch, which was then placed on the skin surface for 15 minutes. After exposure, the stratum corneum (the outer layer of the skin) was gradually removed using 20 adhesive strips, each corresponding to a specific depth within the skin. The concentration of 4-cyanophenol in each stripped layer was quantitatively measured using attenuated total reflectance Fourier transform infrared (ATR-FTIR) spectroscopy, a non-destructive and sensitive technique for detecting chemical compounds within biological tissues. The results of this experiment are shown as discrete points in Fig 3.1, and serve as a reference for comparing the accuracy of classical and fractional diffusion models.

The conditions applied in the experiment are:

$$\begin{cases} C(0,t) = KC_{\text{veh}}, & t > 0. \\ C(h,t) = 0, & t > 0. \\ C(x,0) = 0, & 0 \leq x \leq L. \end{cases}$$

where

- c_{veh} : the concentration of 4-cyanophenol solution in the vehicle.
- K: Distribution coefficient between the stratum corneum and the vehicle.

For the Fickian model(classical model), we represent the well-known solution (2.4)using the following inputs:

- $c_{veh} = 196\,\text{mmol}\,\text{L}^{-1}$.
- $t = 900\,\text{second}$.
- $D = 9.90 \times 10^{-5}\,\text{s}^{-1}$.
- $K = 7.4$.

These values were chosen in accordance with typical experimental conditions [3]. Based on these parameters, we plotted the continuous curve in Fig 3.1, which represents the solution concentration as a function of the relative position.
As for the dashed curve in Fig 3.1, it represents the solution concentration values from the fractional model (2.17) using a simplified approximation of the Mittag-Leffler function with the fractional order set to $\alpha = 0.9$.

$$E_\alpha(-x) \approx \exp\left(-\frac{x^\alpha}{\Gamma(1+\alpha)}\right). \tag{3.1}$$

This is done to accelerate numerical computations and simplify the model analysis.
This approximation provides acceptable results for moderate values of x and is widely used in numerical applications of fractional models.

3.1.2 Results and Discussion

Fig 3.1 It can be observed that the classical model (the continuous curve) almost does not intersect any experimental data points and decreases more rapidly, which causes it to deviate from the experimental data, especially in the middle of the domain.
In contrast, the fractional model (the dashed curve) intersects the experimental data at five points and follows their general trend, demonstrating a higher ability to represent the slow

diffusion of the compound within the skin.
This reflects the presence of microscopic barriers in the skin, anomalous diffusion, and memory effects.

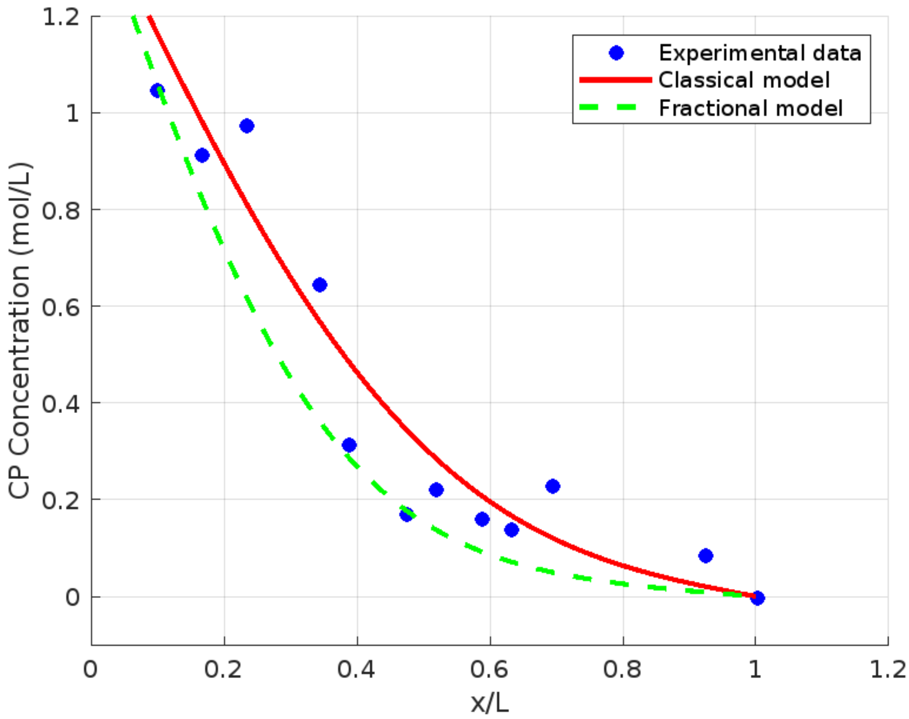

Figure 3.1: Comparison between experimental data and model simulations

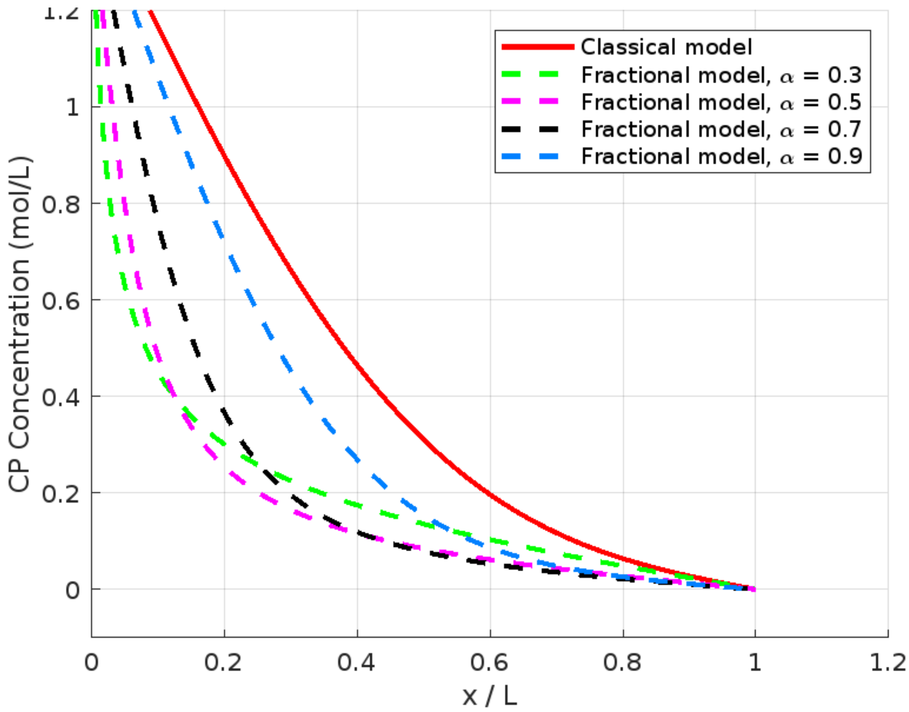

Figure 3.2: Effect of varying the fractional order α on drug concentration in the skin

To study the effect of the fractional derivative on drug diffusion within the skin, several different values of the fractional order α=[1.0 0.9 0.7 0.5 0.3] were used.

Fig 3.2 above shows that lower values of α (such as 0.3 and 0.5) lead to a decrease in the compound concentration in the deeper layers of the skin, indicating a slowdown in the diffusion of the substance within the tissue. This behavior reflects the nature of anomalous diffusion, where molecules do not move freely as in the classical model, but instead their movement is constrained by memory effects and temporal accumulation.

The flexibility in choosing α allows researchers to adjust the model to match different skin conditions, such as dry, or lipid-rich skin, thus enabling the creation of a customized model for a specific biological case. This concept can also be extended to represent temporal changes in skin properties, such as those caused by aging or disease, through the dynamic adjustment of the α value over time or with changing physiological states. Finally, in situations where experimental data is limited or unavailable, α can be used as a tunable parameter, adjusted based on known material or environmental properties. This provides the researcher with a predictive and flexible tool to accurately describe diffusion behavior within the skin.

3.2 Second Model (Interactions between Tilapia Fish and Pelicans

3.2.1 Numerical Solution

For the numerical study of Model (2.18), we approximate the derivative using forward differences, which are defined by the following expression:

$$\left.\frac{dy}{dt}\right|_{t=t_n} \approx \frac{y_{n+1} - y_n}{\Delta t}. \tag{3.2}$$

Let y_n and y_{n+1} denote the values of y at discrete time points t_n and $t_{n+1} = t_n + \Delta t$, respectively, where Δt is the time step size (discretization interval).
By substituting the forward finite difference approximation, we obtain:

$$\begin{cases} S_{n+1} &= S_n + \Delta t \left[r_1 S_n \left(1 - \dfrac{S_n + I_n}{k_1} \right) - \lambda S_n I_n - \dfrac{p_1 S_n^2 Y_n}{1 + S_n + \theta I_n} \right], \\ I_{n+1} &= I_n + \Delta t \left[\lambda S_n I_n - \dfrac{p_2 I_n^2 Y_n}{1 + S_n + \theta I_n} - \gamma I_n \right], \\ Y_{n+1} &= Y_n + \Delta t \left[r_2 Y_n \left(1 - \dfrac{Y_n}{k_2 + S_n + m I_n} \right) + \dfrac{\sigma_1 p_1 S_n^2 Y_n}{1 + S_n + \theta I_n} - \dfrac{\sigma_2 p_2 I_n^2 Y_n}{1 + S_n + \theta I_n} \right]. \end{cases} \tag{3.3}$$

In the fractional case, the Caputo derivative is approximated by the L1 method at t_n

$$^{C}D_t^{\alpha} f(t_n) \approx \frac{1}{\Gamma(2-\alpha)} \sum_{j=0}^{n-1} \frac{1}{\Delta t^{\alpha}} \left[f(t_{j+1}) - f(t_j)\right] \left[(n-j)^{1-\alpha} - (n-j-1)^{1-\alpha}\right].$$

For each of S(t), I(t), and Y(t), we approximate their derivatives using the previously mentioned L1 method, thus obtaining a discretized system:

$$\begin{cases} \dfrac{1}{\Gamma(2-\alpha)} \displaystyle\sum_{j=0}^{n-1} \dfrac{S_{j+1}-S_j}{\Delta t^{\alpha}} w_{n-j} = r_1^{\alpha} S_n \left(1 - \dfrac{S_n + I_n}{k_1}\right) - \lambda^{\alpha} S_n I_n - \dfrac{p_1^{\alpha} S_n^2 Y_n}{1 + S_n + \theta I_n}, \\ \dfrac{1}{\Gamma(2-\alpha)} \displaystyle\sum_{j=0}^{n-1} \dfrac{I_{j+1}-I_j}{\Delta t^{\alpha}} w_{n-j} = \lambda^{\alpha} S_n I_n - \dfrac{p_2^{\alpha} I_n^2 Y_n}{1 + S_n + \theta I_n} - \gamma^{\alpha} I_n, \\ \dfrac{1}{\Gamma(2-\alpha)} \displaystyle\sum_{j=0}^{n-1} \dfrac{Y_{j+1}-Y_j}{\Delta t^{\alpha}} w_{n-j} = r_2^{\alpha} Y_n \left(1 - \dfrac{Y_n}{k_2 + S_n + m I_n}\right) + \sigma_1 \dfrac{p_1^{\alpha} S_n^2 Y_n}{1 + S_n + \theta I_n} - \sigma_2 \dfrac{p_2^{\alpha} I_n^2 Y_n}{1 + S_n + \theta I_n}, \end{cases} \tag{3.4}$$

where the weights are given by:

$$w_{n-j} = (n-j)^{1-\alpha} - (n-j-1)^{1-\alpha}.$$

The resulting nonlinear system is solved numerically employing the Newton-Raphson method. We selected parameter values based on ecological studies of tilapia and pelicans in the Salton Sea,as reported in reference [6].(See tables below)

To display the results of the fractional model behavior and the classical model, we solve both

Parameter	Value
r_1	1.8
r_2	0.0015
k_1	50
k_2	20
p_1	0.05
p_2	0.05
σ_1	0.35
σ_2	0.15
γ	0.24
θ	6
m	0.25
λ	0.06

Table 3.1: Parameter Values Used in the Model

systems (3.3) and (3.4) in MATLAB using the previous variable values and initial conditions ((S,I,Y)=(10,3.5,1.5)).

3.2.2 Results and Discussion

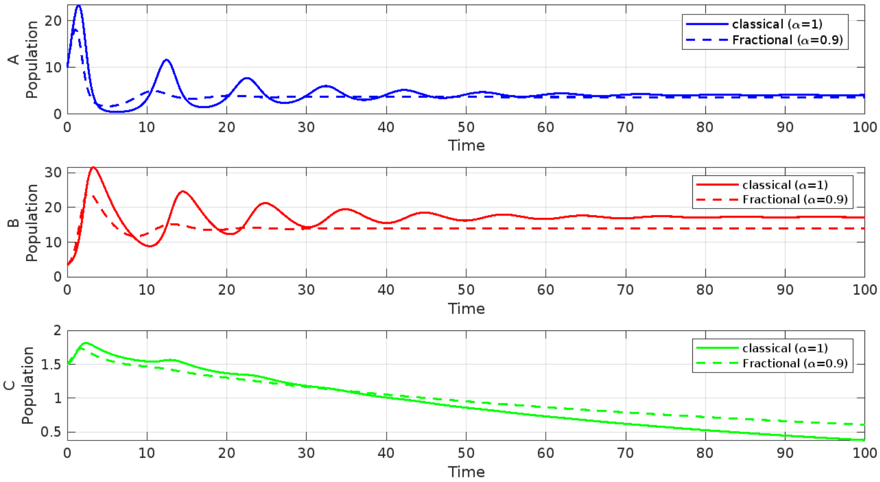

Figure 3.3: Comparison of traditional and fractional models

Figure 3.3 illustrates the behavioral dynamics of susceptible prey, infected prey, and predators under both classical (integer-order) and fractional-order derivatives,where we observe:

- **Panel A**: In the classical model, the number of healthy prey decreases sharply due to the immediate interaction with infection and predation, with persistent oscillations until reaching a stable state. In contrast, in the fractional model, the change in the number of healthy individuals occurs more slowly and smoothly, resulting from the temporal accumulation of infection and predation history, such as the virus incubation periods and the behavioral adaptation of prey by avoiding areas where the disease is widespread.

- **Panel B**: The classical model shows an initial exponential increase in the number of infected prey, indicating rapid disease transmission, followed by a sudden collapse in the population due to predation pressure and infection-induced mortality, with persistent oscillatory behavior. In contrast, the fractional model exhibits a much slower disease spread, thanks to memory effects through resulting from the development of immune responses and the avoidance of disease-spread areas and infected prey, based on cumulative experience.

- **Panel C**: In the initial time period, the number of predators increases in both models due to the abundant availability of both healthy and infected prey. In the classical model, a rapid decrease in predator numbers occurs because it depends solely on the current state of the system. In contrast, in the fractional model, the predator numbers decrease more slowly due to the memory effect, which takes into account periods of nutritional sufficiency and cumulative past influences.

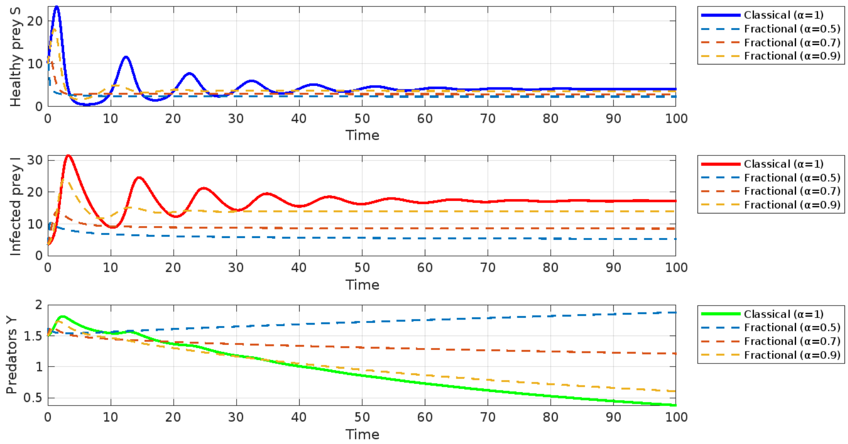

Figure 3.4: Effect of fractional derivative order on the dynamics of prey and predator populations

Fig 3.4 illustrates the effect of varying the fractional derivative order α on the behavior of a predator-prey system with an infectious disease among the prey. It is observed that as the value of α approaches zero, the oscillations in the system's dynamic variables decrease, resulting in a slower and smoother response. This behavior is attributed to the increasing memory effect inherent in the fractional derivative, which leads to a reduction in the infection spread rate. Additionally, a lower α value reduces the predators ability to prey on infected prey, thereby limiting the decline in predator population.

Adjusting the fractional derivative order is considered an effective and essential tool for understanding the characteristics of the biological system and interpreting its dynamic behavior, as well as for predicting its future evolution. By calibrating α based on realistic experimental data, it becomes possible to predict the system's behavior over time with greater accuracy, in addition to inferring information about missing time intervals or incomplete experimental data. Thus, the fractional model contributes to improving the analysis of biological phenomena and providing more precise insights into their development.

CONCLUSIONS

This thesis aims to highlight the motivations that led mathematicians to resort to fractional differential equations in modeling biomedical phenomena, as an alternative to classical differential equations, by pointing out the limitations of the latter in representing complex systems in this field.
In the first chapter, the definitions of fractional derivatives and fractional differential equations were addressed, along with a review of analytical and numerical methods used to solve them. The second chapter focused on the application of fractional equations to two biomedical modeling cases: drug diffusion through the skin, and the predator-prey interaction with infection among the prey, with a comparison between each fractional model and its classical counterpart.The third chapter dealt with numerical simulations using MATLAB to analyze the behavior of the solutions and to identify the differences between the two models: the fractional and the classical.
Based on this study, it can be concluded that fractional differential equations are a powerful and effective tool in biomedical modeling, as they provide higher accuracy and better agreement with real-world data. In addition, they are capable of representing memory effects, time delays, and non-Gaussian behavior, giving them greater predictive power in complex systems.
This thesis marked a turning point in my understanding of the integration between mathematics and biomedical sciences, and confirmed that fractional calculus is not just an abstract mathematical concept, but a valuable tool for a deeper understanding of biomedical phenomena.
Despite the challenges I faced due to the novelty of the subject for me, these obstacles pushed me to develop my research and analytical skills. I hope this work will be a first step toward more advanced research projects in fractional biomedical modeling, whether by improving current models or developing new ones for other systems in the field.

BIBLIOGRAPHY

[1] Balachandran, K. (2023). *An introduction to fractional differential equations (Industrial and Applied Mathematics)*. India.

[2] Brauer, F., & Castillo-Chavez, C. (2012). *Mathematical models in epidemiology*. Springer, New York.

[3] Caputo, M., & Cametti, C. (2020). Diffusion through skin in the light of a fractional derivative approach: Progress and challenges. *Journal of Pharmacokinetics and Pharmacodynamics*.

[4] Cukić, M., & Galović, S. (2023). Mathematical modeling of anomalous diffusive behavior in transdermal drug delivery including time-delayed flux concept. Elsevier.

[5] Diethelm, K. (2004). *The analysis of fractional differential equations*. Springer-Verlag.

[6] Domínguez-Alemán, A., et al. (2024). A predator-prey fractional model with disease in the prey species. *Mathematical Biosciences and Engineering*.

[7] Elias, P. M. (2005). Stratum corneum defensive functions: An integrated view. *Journal of Investigative Dermatology*.

[8] Gorenflo, R., & Mainardi, F. (2000). Fractional calculus: Integral and differential equations of fractional order. *CISM Lecture Notes*.

[9] Jin, B. (2021). *Fractional differential equations*. London, UK: March.

[10] Kilbas, A. A., Srivastava, H. M., & Trujillo, J. J. (2006). *Theory and applications of fractional differential equations*. Elsevier Science.

[11] Mondal, S., et al. (n.d.). Analysis of a fractional order eco-epidemiological model with prey infection and type II functional response. Centre for Mathematical Biology and Ecology, Department of Mathematics, Jadavpur University.

[12] Moustafa, M., Mohd, M. H., Ismail, A. I., & Abdullah, F. A. (2020). Dynamical analysis of a fractional-order eco-epidemiological model with disease in prey population.

[13] Murray, J. D. (2002). *Mathematical biology I: An introduction* (3rd ed.). Springer.

[14] Podlubny, I. (1999). *Fractional differential equations*. San Diego: Academic Press.

[15] Prausnitz, M. R., Mitragotri, S., & Langer, R. (2004). Current status and future potential of transdermal drug delivery. *Nature Reviews Drug Discovery*.

[16] Sharma, S., et al. (2017). Mathematical modeling and analysis of predator–prey interactions with disease in prey population. *Nonlinear Dynamics*.

[17] Stewart, J. (2016). *Calculus: Early transcendentals* (8th ed.). Brooks Cole.

[18] Tellab, B. (2018). *Fractional differential equations* (PhD thesis). Mentouri Brothers University Constantine-1.

[19] West, B. J. (2003). *Fractional calculus view of complexity: Tomorrow's science*. CRC Press.

Appendix A: Auxiliary Mathematical Definitions

- $\Gamma(x)$:Generalizing the factor to complex numbers is called **gamma function** . It is defined for $\Re(x) > 0$ by Euler's integral:

$$\Gamma(x) = \int_0^\infty t^{x-1} e^{-t}\, dt.$$

It satisfies the recurrence relation:

$$\Gamma(x+1) = x\Gamma(x) \qquad\qquad \Gamma(n) = (n-1)! \quad n \in \mathbb{N}^*.$$

- $\beta(x,y)$: The **Beta function**, denoted as $\beta(x,y)$, is defined by the following integral:

$$\beta(x,y) = \int_0^1 t^{x-1}(1-t)^{y-1}\, dt$$

for $x, y > 0$. It is symmetric, meaning $\beta(x,y) = \beta(y,x)$, and is related to the Gamma function by the identity:

$$\beta(x,y) = \frac{\Gamma(x)\Gamma(y)}{\Gamma(x+y)}$$

- $E_{\alpha,\beta}(x)$: The **Mittag-Leffler function** is defined as:

$$E_{\alpha,\beta}(x) = \sum_{n=0}^{\infty} \frac{x^n}{\Gamma(\alpha n + \beta)} \qquad \alpha > 0 \quad \beta \in \mathbb{C}.$$

where:

  - x is the argument of the function,
  - $\Gamma(x)$ is the Gamma function.

$$E_{1,1}(x) = \sum_{n=0}^{\infty} \frac{x^n}{n!} = e^x$$

(This is just the standard exponential function.)

- $(f * g)(x)$: The **convolution** between $f(x)$ and $g(x)$, $(f * g)(x)=\int_{-\infty}^{\infty} f(t)g(x-t)\, dt$.

- $\mathcal{L}\{f(x)\}(s)$:The **Laplace transform** of a function $f(x)$,$\mathcal{L}\{f(x)\}(s) = \int_0^\infty e^{-sx} f(x)\, dx$.
Table of Inverse Laplace Transforms for Basic Functions:

Laplace Transform $\mathcal{L}\{f(x)\}$	**Inverse Laplace Transform** $f(x)$
$\frac{1}{s}$	1
$\frac{1}{s^2}$	x
$\frac{1}{s^n}$	$\frac{x^{n-1}}{(n-1)!}$
$\frac{1}{s+a}$	e^{-ax}
$\frac{1}{s^2+a^2}$	$\frac{1}{a}\sin(ax)$
$\frac{1}{s^2+a^2}$	$\frac{1}{a}\cos(ax)$
$\frac{1}{s^2-a^2}$	$\frac{1}{2a}\sinh(ax)$
$\frac{1}{s^2-a^2}$	$\frac{1}{2a}\cosh(ax)$
$\frac{1}{s}e^{-bx}$	$\frac{1}{s+b}$
$\frac{1}{s^2+\alpha^2}$	$\frac{1}{\alpha}\sin(\alpha x)$
$\frac{1}{s^2-\alpha^2}$	$\frac{1}{\alpha}\sinh(\alpha x)$

Table 2: Common Laplace Transforms and their Inverses

Appendix B: MATLAB Codes

B.1 MATLAB Code for Drug Diffusion through Skin: Classical and Fractional Models

```
% ----- Experimental data -----
x_data = [ ...
0.0994, 0.1670, 0.2346, 0.3439, 0.3877, ...
0.4751, 0.5189, 0.5885, 0.6322, 0.6938, ...
0.9245, 1.0020];
C_data = [ ...
1.0465, 0.9126, 0.9740, 0.6447, 0.3126, ...
0.1702, 0.2205, 0.1591, 0.1367, 0.2288, ...
0.0837, -0.0028];

% ----- Parameters -----
C_veh = 0.196;
K = 7.4;
t = 900;
alpha = 0.9;
D_eff = 9e-05;
N = 100;
h = 1;
xL = linspace(0, 1, 200);

% ----- Mittag-Leffler function approximation -----
approx_ML = @(z,alpha ) exp(-z.^alpha / gamma(1 + alpha));

% ----- Fractional model using Mittag-Leffler approximation -----
C_frac = zeros(size(xL));
for i = 1:length(xL)
sum_series = 0;
for n = 1:N
lambda_n = n * pi;
z = D_eff * (lambda_n^2) * t^alpha;
ML_approx = approx_ML(z, alpha);
term = (2 / (n * pi)) * sin(lambda_n * xL(i)) * ML_approx;
sum_series = sum_series + term;
end
C_frac(i) = K * C_veh * (1 - xL(i) - sum_series);
end
```

```
% ----- Classical model for comparison -----
C_classic = zeros(size(xL));
D_classic = 9e-5;
for i = 1:length(xL)
sum_series = 0;
for n = 1:N
term = (2 / (n * pi)) * sin(n * pi * xL(i)) * exp(-D_classic * n^2 * pi^2 * t);
sum_series = sum_series + term;
end
C_classic(i) = K * C_veh * (1 - xL(i) - sum_series);
end

% ----- Plotting -----
figure;
hold on;
plot(x_data, C_data, 'bo', 'MarkerFaceColor', 'b', 'DisplayName', 'Experimental data
    ');
plot(xL, C_classic, 'r-', 'LineWidth', 2, 'DisplayName', 'Classical model');
plot(xL, C_frac, 'g--', 'LineWidth', 2, 'DisplayName', ['Fractional model ']);
xlabel('x/L');
ylabel('CP Concentration (mol/L)');
legend('Location', 'northeast');
xlim([0 1.2]);    % Limit x-axis from 0 to 1
ylim([-0.1 1.2]); % Limit y-axis from 0 to 1.2
grid on;
```

B.2 MATLAB Code for Solving Classical and Fractional Predator–Prey Model with Infectious Disease

```
% Basic parameters from the table
r1 = 1.8;
r2 = 0.0015;
k1 = 50;
k2 = 20;
p1 = 0.05;
p2 = 0.05;
sigma1 = 0.35;
sigma2 = 0.15;
gamma_val = 0.24;
theta = 6;
```

```
m = 0.25;
lambda = 0.06;
% Initial conditions
S0 = 10;
I0 = 3.5;
Y0 = 1.5;
% Simulation time settings
t_start = 0;
t_end = 100;
dt = 0.1;
N = round((t_end - t_start)/dt);
t = linspace(t_start, t_end, N+1);

% Solve classical model (alpha=1)
alpha_trad = 1;
[S_trad, I_trad, Y_trad] = solve_model(alpha_trad, r1, r2, k1, k2, p1, p2, ...
sigma1, sigma2, gamma_val, ...
theta, m, lambda, S0, I0, Y0, t, dt);

% Solve fractional model (alpha=0.9)
alpha_frac = 0.9;
[S_frac, I_frac, Y_frac] = solve_model(alpha_frac, r1, r2, k1, k2, p1, p2, ...
sigma1, sigma2, gamma_val, ...
theta, m, lambda, S0, I0, Y0, t, dt);

% Display comparison results with modified plot function
plot_comparison(t, S_trad, I_trad, Y_trad, S_frac, I_frac, Y_frac);

function [S, I, Y] = solve_model(alpha, r1, r2, k1, k2, p1, p2, ...
sigma1, sigma2, gamma_val, ...
theta, m, lambda, S0, I0, Y0, t, dt)
% Modify parameters according to fractional order
if alpha < 1
r1_a = r1^alpha;
r2_a = r2^alpha;
p1_a = p1^alpha;
p2_a = p2^alpha;
gamma_a = gamma_val^alpha;
lambda_a = lambda^alpha;
else
r1_a = r1;
```

```
r2_a = r2;
p1_a = p1;
p2_a = p2;
gamma_a = gamma_val;
lambda_a = lambda;
end

% Time-independent parameters remain unchanged
k1_a = k1;
k2_a = k2;
sigma1_a = sigma1;
sigma2_a = sigma2;
theta_a = theta;
m_a = m;

% Initialize arrays
N = length(t)-1;
S = zeros(1, N+1);
I = zeros(1, N+1);
Y = zeros(1, N+1);
S(1) = S0;
I(1) = I0;
Y(1) = Y0;

if alpha < 1
weights = zeros(1, N+1);
weights(1) = 1;
for j = 1:N
weights(j+1) = (1 - (1+alpha)/j)*weights(j);
end

for n = 1:N
denom = 1 + S(n) + theta_a * I(n);

dS = r1_a * S(n) * (1 - (S(n) + I(n))/k1_a) ...
- lambda_a * S(n) * I(n) ...
- p1_a * S(n)^2 * Y(n) / denom;

dI = lambda_a * S(n) * I(n) ...
- p2_a * I(n)^2 * Y(n) / denom ...
- gamma_a * I(n);
```

```
dY = r2_a * Y(n) * (1 - Y(n)/(k2_a + S(n) + m_a * I(n))) ...
+ sigma1_a * p1_a * S(n)^2 * Y(n) / denom ...
- sigma2_a * p2_a * I(n)^2 * Y(n) / denom;

sum_S = sum(weights(2:n+1).*(S(n:-1:1) - S0));
sum_I = sum(weights(2:n+1).*(I(n:-1:1) - I0));
sum_Y = sum(weights(2:n+1).*(Y(n:-1:1) - Y0));

S(n+1) = S0 + (dt^alpha * dS - sum_S)/weights(1);
I(n+1) = I0 + (dt^alpha * dI - sum_I)/weights(1);
Y(n+1) = Y0 + (dt^alpha * dY - sum_Y)/weights(1);

S(n+1) = max(S(n+1), 0);
I(n+1) = max(I(n+1), 0);
Y(n+1) = max(Y(n+1), 0);
end
else
% Classical solution using Euler's method
for n = 1:N
denom = 1 + S(n) + theta * I(n);

dS = r1 * S(n) * (1 - (S(n) + I(n))/k1) ...
- lambda * S(n) * I(n) ...
- p1 * S(n)^2 * Y(n) / denom;

dI = lambda * S(n) * I(n) ...
- p2 * I(n)^2 * Y(n) / denom ...
- gamma_val * I(n);

dY = r2 * Y(n) * (1 - Y(n)/(k2 + S(n) + m * I(n))) ...
+ sigma1 * p1 * S(n)^2 * Y(n) / denom ...
- sigma2 * p2 * I(n)^2 * Y(n) / denom;

S(n+1) = S(n) + dt * dS;
I(n+1) = I(n) + dt * dI;
Y(n+1) = Y(n) + dt * dY;

S(n+1) = max(S(n+1), 0);
I(n+1) = max(I(n+1), 0);
Y(n+1) = max(Y(n+1), 0);
```

```
end
end
end

% Modified plot_comparison function
function plot_comparison(t, S_trad, I_trad, Y_trad, S_frac, I_frac, Y_frac)
figure('Name', 'sa', ...
'NumberTitle', 'off', 'Position', [100, 100, 1000, 800]);

% Healthy prey S
subplot(3,1,1);
plot(t, S_trad, 'b-', 'LineWidth', 1.5, 'DisplayName', 'classical (\alpha=1)');
hold on;
plot(t, S_frac, 'b--', 'LineWidth', 1.5, 'DisplayName', 'Fractional (\alpha=0.9)');
ylabel({'A', 'Population'});
xlabel('Time');
legend('Location', 'best');
grid on;
hold off;

% Infected prey I
subplot(3,1,2);
plot(t, I_trad, 'r-', 'LineWidth', 1.5, 'DisplayName', 'classical (\alpha=1)');
hold on;
plot(t, I_frac, 'r--', 'LineWidth', 1.5, 'DisplayName', 'Fractional (\alpha=0.9)');
ylabel({'B', 'Population'});
xlabel('Time');
legend('Location', 'northeast');
grid on;
hold off;
% Predators Y
subplot(3,1,3);
plot(t, Y_trad, 'g-', 'LineWidth', 1.5, 'DisplayName', 'classical (\alpha=1)');
hold on;
plot(t, Y_frac, 'g--', 'LineWidth', 1.5, 'DisplayName', 'Fractional (\alpha=0.9)');
xlabel('Time');
ylabel({'C', 'Population'});
legend('Location', 'northeast');
grid on;
hold off;
end
```

الملخص

تستعرض هذه المذكرة دور المعادلات التفاضلية الكسرية في نمذجة الظواهر الطبية الحيوية التي تتميز بخصائص الذاكرة والسلوك غير الغاوسي. تبدأ بعرض أساسيات الحساب الكسري وطرق حل المعادلات التفاضلية الكسرية، ثم تقدم نموذجين بيولوجيين بصيغتهما الكلاسيكية والكسرية. تختتم الدراسة بإجراء محاكاة عددية لسلوك كل نموذج باستخدام برنامج ماتلاب، مع تحليل تأثير تغيير رتبة المشتقة الكسرية على ديناميكية النظام. تظهر النتائج تفوق النماذج الكسرية في تمثيل الأنظمة الحيوية المعقدة بمرونة وواقعية أكبر.

الكلمات المفتاحية: المعادلات التفاضلية الكسرية، المشتقة الكسرية لكابوتو، النمذجة الطبية الحيوية، تأثير الذاكرة.

Abstract

This thesis examines the role of fractional differential equations in modeling biomedical phenomena characterized by memory properties and non-Gaussian behavior. It begins with an overview of the fundamentals of fractional calculus and methods for solving fractional differential equations, then presents two biological models in both their classical and fractional forms. The study concludes with numerical simulations of each model's behavior using MATLAB, analyzing the impact of varying the fractional derivative order on the system dynamics. The results demonstrate the superiority of fractional models in representing complex biomedical systems with greater flexibility and realism.

Keywords: Fractional differential equations, Caputo fractional derivative, biomedical modeling, memory effect.

Résumé

Ce mémoire examine le rôle des équations différentielles fractionnaires dans la modélisation des phénomènes biomédicaux caractérisés par des propriétés de mémoire et un comportement non gaussien. Il commence par une présentation des fondamentaux du calcul fractionnaire et des méthodes de résolution des équations différentielles fractionnaires, puis présente deux modèles biologiques sous leurs formes classique et fractionnaire. L'étude se conclut par des simulations numériques du comportement de chaque modèle à l'aide de MATLAB, analysant l'impact de la variation de l'ordre de la dérivée fractionnaire sur la dynamique du système. Les résultats démontrent la supériorité des modèles fractionnaires dans la représentation des systèmes biomédicaux complexes avec une plus grande flexibilité et réalisme.

Mots-clés : Équations différentielles fractionnaires, dérivée fractionnaire de Caputo, modélisation biomédicale, effet de mémoire.